DTU Aqua
National Institute of Aquatic Resources

New tools to assess the environmental effects of mussel dredging

Camille Saurel, Kasper Andersen, Pascal Barreau, Marie Maar, Ane Pastor, Janus Larsen, Christian Mohn, Jens Murawski, Jun She and Jens Kjerulf Petersen

DTU Aqua Report no. 390-2021

DTU Aqua
National Institute of Aquatic Resources

New tools to assess the environmental effects of mussel dredging

Camille Saurel[1], Kasper Andersen[1], Pascal Barreau[1], Marie Maar[2], Ane Pastor[2], Janus Larsen[2], Christian Mohn[2], Jens Murawski[3], Jun She[3] and Jens Kjerulf Petersen[1]

[1] DTU Aqua, Technical University of Denmark
[2] Aarhus University, AU
[3] Danish Meteorological Institute, DMI

DTU Aqua Report no. 390-2021

Colophon

Title:	New tools to assess the environmental effects of mussel dredging
Authors:	Camille Saurel[1], Kasper Andersen[1], Pascal Barreau[1], Marie Maar[2], Ane Pastor[2], Janus Larsen[2], Christian Mohn[2], Jens Murawski[3], Jun She[3] and Jens Kjerulf Petersen[1]
	[1] DTU Aqua, Technical University of Denmark [2] Aarhus University, AU [3] Danish Meteorological Institute, DMI
DTU Aqua Report no.:	390-2021
Year:	Scientific work finalized May 2021. Report published November 2021
Reference:	Saurel, C., Andersen, K., Barreau, P. Maar, M., Pastor, A., Larsen, J., Mohn, C., Murawski, J., She, J. & Petersen, J.K (2021). New tools to assess the environmental effects of mussel dredging. DTU Aqua Report no. 390-2021. National Institute of Aquatic Resources, Technical University of Denmark, 55 pp.
Quality assurance:	The report has been peer reviewed by Anja Skjoldborg Hansen and Hans Jakobsen, Aarhus University, and Jørgen Dalsskov, DTU Aqua. The peer reviewers have not been part of the project
Cover photo:	Rinsing of mussel dredges, Limfjorden, Denmark © Camille Saurel, DTU Aqua
Published by:	National Institute of Aquatic Resources, Øroddevej 80, 7900 Nykøbing Mors, Denmark
Download:	www.aqua.dtu.dk/publikationer
ISSN:	1395-8216
ISBN:	978-87-7481-313-2

DTU Aqua Reports contain results from research projects, reviews of specific topics, expositions for authorities etc.

Preface

This project has received financial support from the European Maritime and Fisheries Fund and the Danish Foreign Ministries development program for fisheries. The topic of the report has been a result of discussions in the Danish Mussel Committee that is an advisory body for management of the oyster and mussel fisheries in Danish waters-

Nykøbing Mors, May 2019

Camille Saurel & Jens Kjerulf Petersen

DTU Aqua
Dansk Skaldyrcenter,
Øroddevej 80
7900 Nykøbing Mors
Tlf.: 96 69 02 83
post@skaldyrcenter.dk
www.aqua.dtu.dk/forskning/skaldyr

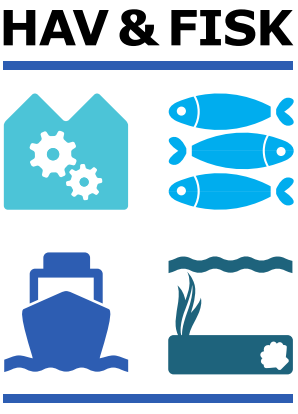

Content

Summary

In order to improve the scientific basis for public management of mussel and oyster fisheries, it is the purpose of this investigation to develop new knowledge about the indirect effects on the marine environment of mussel and oyster dredging activities, and in particular to develop new tools and methods to assess the indirect fishery effects at the level of entire basins. Three main topics are studied: The extension and duration of sediment plumes caused by resuspension of sediments due to mussel dredging, the effects of transplantation of mussels from areas frequently exposed to oxygen depletion and links between fishery and recruitment of new spat to mussel beds.

Sediment plumes created by dredging was studied as a combination of in situ experiments in Lovns Bredning and Løgstør Bredning in the Limfjorden, Denmark. In the field experiments, mussel fishermen dredged along specified tracks or in predefined areas, and water properties like light extinction, oxygen consumption, hydrodynamic conditions and turbidity were measured in relation to fishing intensity. Further, sediment characteristics of the test area were determined. Data from the field experiments were fed into a new sediment resuspension and plume dispersion model included in a newly established FlexSem framework model of the Limfjorden with a spatial resolution of 10 m in the studied areas. The FlexSem framework was coupled to a new hydrodynamic version of DMI's ocean model HBM that had been expanded with a Limfjorden domain, and new modules were added. This new hydrodynamic setup enhances the forecasting capabilities from sea level predictions to forecasts of all physical ocean parameters with reasonably good quality predictions of temperatures, salinity and currents in high temporal and spatial resolution. Results showed that the plume has an extension of 260-540 m from the dredge track and with a duration of approximately one h. Results showed that the plume has an extension of 260-540 m from the dredge track and with a duration of approximately one h. The plume's extension depends on the sediment characteristics of the fished area defined by grain size distribution, hydrodynamic conditions and fishing intensity. In the scenario setting, it was decided to apply conservative estimates so the model results can be assumed to be the worst case.

The effects of mussel transplantations from areas often exposed to oxygen depletion were studied as a combination of laboratory experiments determining oxygen consumption of decaying mussels and 3D coupled hydrodynamic-biochemical model, including hypoxia development of Lovns Bredning using the FlexSem framework. Based on data from the industries current relay praxis, scenarios of removal of 3600 and 6000 t mussel respectively were chosen as realistic. Modelled results showed that the transplantations on a short-term scale increased oxygen concentrations and reduced nutrient and Chl a concentration in the water column on a long-term scale. There was an immediate negative effect on mussel biomass but post the oxygen depletion, remaining mussels grew faster and thus compensated for the removed mussels.

Field experiments measuring mussel recruitment on the bottom and in the water column on five different locations with fished vs un-fished plots could not demonstrate a direct link between mussel recruitment and fisheries. However, the field experiment suggested that the thinning of the mussel beds promoted growth measured as shell length of the remaining mussels. We suggest that this result combined with the analysis of fishery data could explain that fishery promotes growth in remaining mussel, making the beds sustain fisheries for 2-3 years under the current fishing pressure. A modelling approach was used to study the mussel larvae dispersal, and the connectivity between the different broads of the Limfjorden using an Agent Based Model and the Limfjorden physical model. Modelled results indicated that mussel larvae were present in most of the broads, and this was validated by *in situ* measurement of mussel recruitment in the water column. Field measurements results indicated that many mussel larvae were recruited in the water column, but failed to recruit at the bottom. This

confirms the complexity of the bottom mussel recruitment dynamic where other factors such as predators, intra and inter-competition for space and food reduce the chances of spat survival.

Following to the Danish mussel policy direction on improving mussel management, the presented results were used as background for new management recommendations. Modelling and field measurements showed that the sediment plume produced by mussel fishing activity extended 260-540m away from the dredge track and could last up to 1h in the water column. The modelled cumulative sedimentation from fishery events was below natural sedimentation. Together with the given low fishing activities (number of boats and fishing days per year) near the eelgrass boxes in Lovns Bredning, sedimentation was not considered as an indirect negative effect on eelgrass growth and development. Therefore, it was recommended to reduce the eelgrass boxes buffer from 300 m to 100 m in the management plans of Lovns bredning. Hence, a buffer between these zones is defined as protection against physical damage rather than indirect effects from resuspended sediment. Accordingly, for the fishing season 2020-2021, the buffer zone was reduced to 100m in the study area. It is further recommended that management include positive effects when considering permits for mussel transplantations from eutrophic ecosystem with frequent hypoxia, where removal of mussel biomass by mussel fishery could be used as hypoxia mitigation tool to improve water quality.

1. Introduction

Dredging for mussels and oysters has some immediate and easily measurable effects on the areas of the seabed that are directly affected by the dredge. These effects have received increased attention in recent years, e.g. in relation to the implementation of various EU environmental directives, where the focus of the environmental impact of fisheries are less on the target species and more on the ecosystem. However, there are other more indirect effects of the fisheries, which may still potentially affect the environment and depend on the local environmental conditions. These effects may be related to other effects on the bottom, e.g. in the form of resuspension of sediment caused by the fishing gear, which affects the light climate and thus the benthic vegetation. In eutrophic areas, such additional impact on light attenuation may be critical to the key ecosystem components like eelgrass and macroalgae and thus further limit their propagation and condition.

Government agencies managing the mussel and oyster fisheries are thus obliged to include all environmental drivers when mapping impacts of fishing. In the coastal zone, the fishery must comply with environmental and nature conservation goals set by the EU Water Framework Directive and EU Species and Habitats Directive. At present, the management objectives and principles for mussel and oyster fishery are stated in the Danish mussel policy (https://fiskeristyrelsen.dk/media/10650/muslinge-og-oesterspolitik.pdf, in Danish) that is balanced between utilization of the shellfish resource and protection of key ecosystem components like eelgrass, macroalgae and benthic fauna from the direct physical damage caused by the dredging as well as potential indirect effects. However, at present, there is little knowledge on the indirect effects of mussel dredging. As a consequence, the management either does not consider the indirect effects and thus does not meet the intentions of the Common Fisheries Policy to protect the marine environment, e.g. in relation to the implementation of the Water Framework Directive (2000/60/EC), or that the management becomes too restrictive according to the precautionary principle and hence, in fact, does not live up to the intentions of the Common Fisheries Policy to increase productivity and profitability in the industry. Thus, knowledge of the direct and indirect effects of fishing is therefore of great importance to the fisheries' management and the industry. We used the Limfjorden in Denmark as a case study (figure 1.1)

The effects of mussel fishery are not entirely negative on the environment. Recent studies (Dinesen et al., 2015) have shown that closure of areas can subsequently affect the mussel beds so that the mussels disappear from an area closed to fishing. Likewise, it has been found that mussel fishing takes place to a very large extent at the same fishing grounds, which indicates that the mussel fishing itself can contribute to maintaining the mussel beds. Loss of mussel beds is not unproblematic to the environmental condition in the coastal areas because the mussels' filtration of the water helps to limit the phytoplankton biomass, e.g. measured as the concentration of chlorophyll. In other aspects, mussel fishery may potentially also improve general environmental conditions in eutrophic areas. Large parts of Danish coastal areas are often affected by oxygen depletion, which is particularly the case in the Limfjorden. By removing mussel biomass from the bottom in areas that are about to be exposed to oxygen depletion, fishing may help reduce the extent of oxygen depletion due to biomass decay, while saving valuable resources.

The present project aims to develop new knowledge about the indirect effects on the marine environment of mussel and oyster dredging activities and develop new tools and methods that can establish new knowledge on fishery affects on the level of entire basins. The tools will be used in coastal waters, where other anthropogenic effects - primarily large inputs from the land of nutrients - are of large importance to general environmental status.

In the present project, the following activities were carried out:

- A 3D coupled sediment resuspension model of the Limfjorden based on data input from in situ experiments were established to determine the importance of resuspension resulting from mussel dredging to light conditions for benthic vegetation such as eelgrass and macroalgae.
- Using both experimental data and a 3D coupled hydrodynamic-biochemical model to estimate the effects of removing mussels from oxygen depleted areas.
- Through practical trials and the industry's activities, determine the importance of mussel dredging for recruitment of blue mussels in the Limfjorden and a 3D physical model for mussel larvae dispersal coupled with an Agent Based Model (ABM) to examine the connectivity between sub-areas in the Limfjorden.

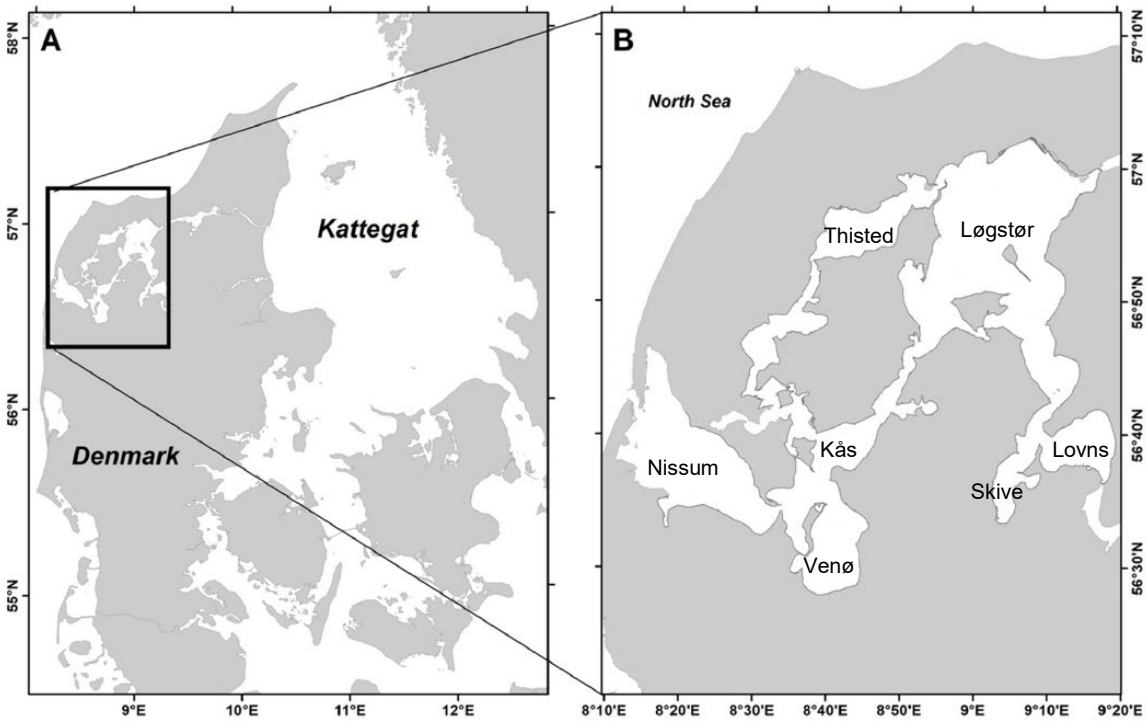

Figure 1.1. Map of Denmark (A) and the western part of Limfjorden (B) with selected broads.

2. Modelling tools – Limfjorden setup[1]

2.1 Physical model

DMI has an almost 20-year history in modelling the Limfjorden. The first two-dimensional (2D) hydrodynamic model-based sea level prediction and storm surge warning service were established 2001 (DMI tech. rep. 01-07). In 2007, improved performance of a full baroclinic, three-dimensional (3D) model in predicting sea level was demonstrated. Hence the 2D hydrodynamic model was replaced by the general circulation model HBM (HIROMB-BOOS-Model[2]), DMI's operational storm surge model (Berg 2012, Berg and Poulsen 2012). The HBM code has been developed and routinely upgraded, but the original Limfjorden set-up in 370 m horizontal resolution is still in operational use. During the past decade, HBM has proven to predict sea level in the Limfjorden very well. Other parameters were assumed to be less well predicted, due to lack of information in near real-time on freshwater runoff and bio-geochemical input from rivers and land sources, other hydrographic parameters (salinity, vertical current structure, sea ice). This type of input was finally obtained from the Swedish E-HYPE model developed by SMHI in 2016, and implemented the same year, enabling forecasts of a wide range of physical ocean parameters.

In the framework of the project, a new set-up in double (185 m ≈ 1/10 nautical mile) horizontal resolution has been developed. For DMI, this is a step towards high resolution modelling for developing near coastal services and applications, in order to address user needs in the highly variable coastal zone (She & Murawski 2018). In the project, DMI provided boundary conditions for a local model which focuses on sediment drift studies at two selected Limfjorden sites: Lovns and Løgstør.

Realistic local, high resolution model application require both, set-ups that are highly enough resolved to cover the local scales in space and time, and boundary forcing from larger, regional-scale models that cover the all the surrounding seas. For the application as a regional scale model in the project, DMI's North Sea and Baltic Sea model HBM has been upgraded to cover the Limfjorden in 185.2 m (1/10-th of a nautical mile) resolution (Figure 2.1). The high resolution Limfjorden area is two-way nested into the North Sea and Baltic Sea, which ensures good quality of the signals propagating into the Limfjorden and the high-quality forecast of the ocean currents in the entire fjord.

[1] This work has been published in: Murawski J, She J, Mohn C, Frishfelds V and Nielsen JW (2021) Ocean Circulation Model Applications for the Estuary-Coastal-Open Sea Continuum.Front. Mar. Sci. 8:657720. doi: 10.3389/fmars.2021.657720
[2] HIROMB is an abbreviation for High Resolution Oceanographic Model for the Baltic. BOOS stands for the Baltic Operational Oceanographic System.

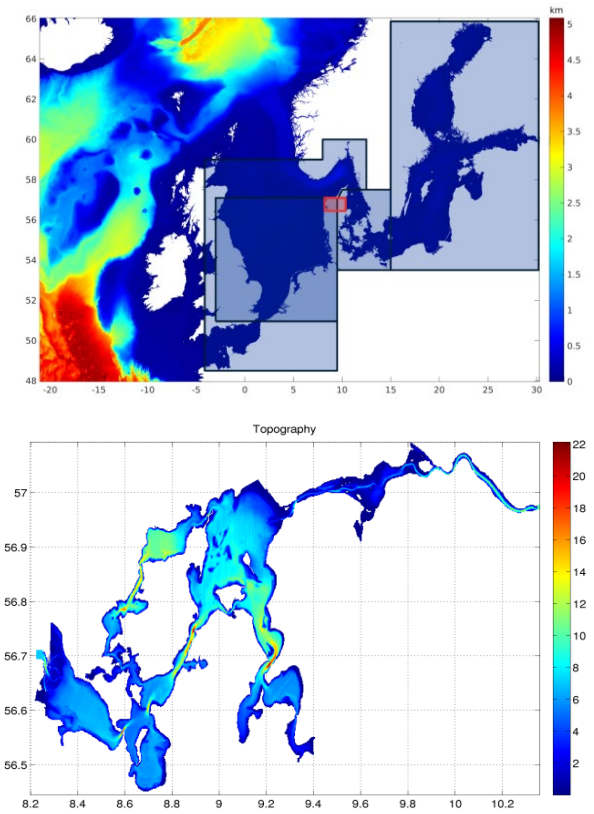

Figure 2.1. Model set-up (left) and Limfjorden bathymetry (right). The set-up has a spatial resolution of 3 n.m. in the North Sea and Baltic Sea, 1 n.m. in the Extended Wadden Sea, 0.5 n.m. in the Danish straits and 185 m resolution in the Limfjorden domain (red box).

The Limfjorden domain is embedded into DMI's regional set-up, connecting to the North Sea in the west and the Kattegat in the east (Figure 2.1, red box), ensures that tidal forcing from the North Sea is included and a strong west-east salinity gradient along the fjord is present. The model was initialized in July 2008 by combining 41 S/T fjord profile measurements with DMI's operational North Sea - Baltic Sea model results. Run-off data for 31 streams and coastal segments in the Limfjorden region were generated using input data from a 30-year E-Hype re-analysis. Weather data from DMI's operational HIRLAM model in approx. 5km resolution (approx. 3km since medio 2009) was used to force the ocean model. A 4+1-year hind cast run for the years 2009 -2012 and 2017 was conducted to provide boundary conditions for the sediment drift studies. Time averaged, mean HBM output files holding one data set every 15 minutes were provided. The volume preserving feature of time averaged output files is essential for drift simulations of suspended materials. For 2017, instantaneous model output files were provided, for a comparison with the monitoring data from the campaign. In between 2012 and 2017, HBM model run in update mode, with reduced time resolution.

DMI provided a 4 year dataset (2009-2012) of time averaged HIRLAM+HBM model output: 10m-wind, currents, salinity, temperature and sea level and a 1-year dataset (2017) of instantaneous model output; for the local drift assessments. The model has been validated using profile salinity and temperature measurements provided by DCE, as well as salinity, temperature and currents measurements from the first monitoring campaign in 2017. During the project, the HBM model and setup were continuously improved to better represent the observations: RMS error of seal level range from 6cm at most western stations, including Løgstør (Figure 2.2) to 10 cm in the Eastern Limfjorden, RMS error of sa-

linity and temperature of less than 2 psu and 0.8°C, respectively, depending on the depth and adequately modelled currents. The challenge is to model the transport through narrow straits, especially the strong currents that occur during storms. Fresh water input by rivers can lead to a freshening of the fjord when the transport of salty North Sea water through the narrow straits is not treated with sufficient accuracy.

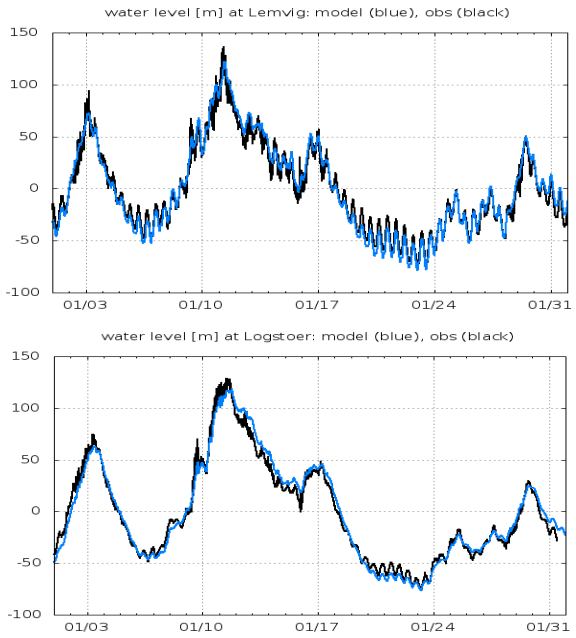

Figure 2.2. Sea level model results (blue) show good agreement with observed values (black), at Lemvig (left) and Løgstør (right). The variability of sea level is well reproduced. RMS errors for a 1-year time series range from 6cm in the western part of the Limfjorden to 10 cm in the eastern Limfjorden. This is within the accepted quality limit of storm surge modelling.

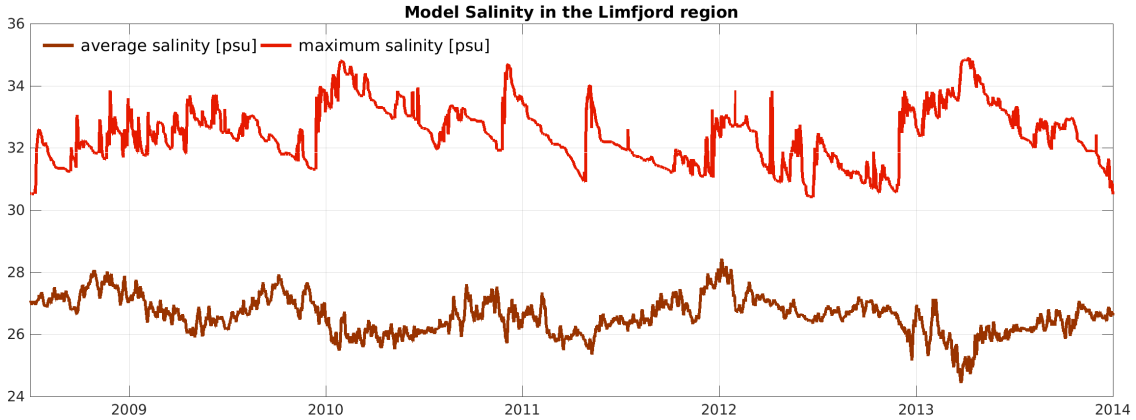

Figure 2.3. Time series of mean (dark red) and maximum (light red) salinity in the Limfjorden. Mean value have been calculated by averaging over grid cells with 2 m thickness at the surface and 1m thickness below the surface.

Figure 2.3 shows the time series of the modelled mean salinity in the Limfjorden in the period July 2008 to December 2013. The results indicate the absence of a clear trend in the salinity, which is what one should expect. To archive this, different river forcing was tested, and the model bathymetry

was tuned to improve the transport through the narrow straits. This tuning also benefitted the propagation of the sea level signals into and inside the fjord. Apart from the model bathymetry, the HBM model has not been tuned specifically for the Limfjorden region. The same parameterizations are used everywhere: in the North Sea and Baltic Sea, as well as in the Limfjorden.

The impact of even higher, horizontal model resolution has been tested using 92.6 m grid spacing in the Limfjorden domain. Salinity RMSE values and biases are largely improved by the resolution increase. Salinity biases in Visby Bredning and Thisted Bredning are 20% to 40% lower (at one location 60% lower). In the central parts, salinity biases decrease by 10% to 20%. For the application in drift modelling of suspended matter, the quality of the drift currents is essential. This is a challenging task for regional model with relative coarse resolution. Factors that determine the model quality are: The quality of the meteorological forcing, the forcing at the boundaries, river forcing (steric effects) and mixing, as well as the set-up of the model, e.g. resolution. A sensible way to evaluate currents is to analyse progressive vector plots (PVP), i.e. to follow the path of one would take if one would flow with the currents at a given location. PVP diagrams accumulate errors along the pathway. Figure 2.4 shows a comparison of modelled and observed currents March 6th to March 10th 2017. There are differences, but the general features are represented and well matched in time. Qualitative Comparison of modelled and measured currents:

1. Surface currents reverse after the 1 day, in the evening of the 7-th of March 2017.
2. North-easterly currents change to south-easterly currents in the night from the 7-th to the 8-th of March 2017, close to midnight.
3. At the 8-th of March 2017, at around noon, the currents in all three layers turn southwest.

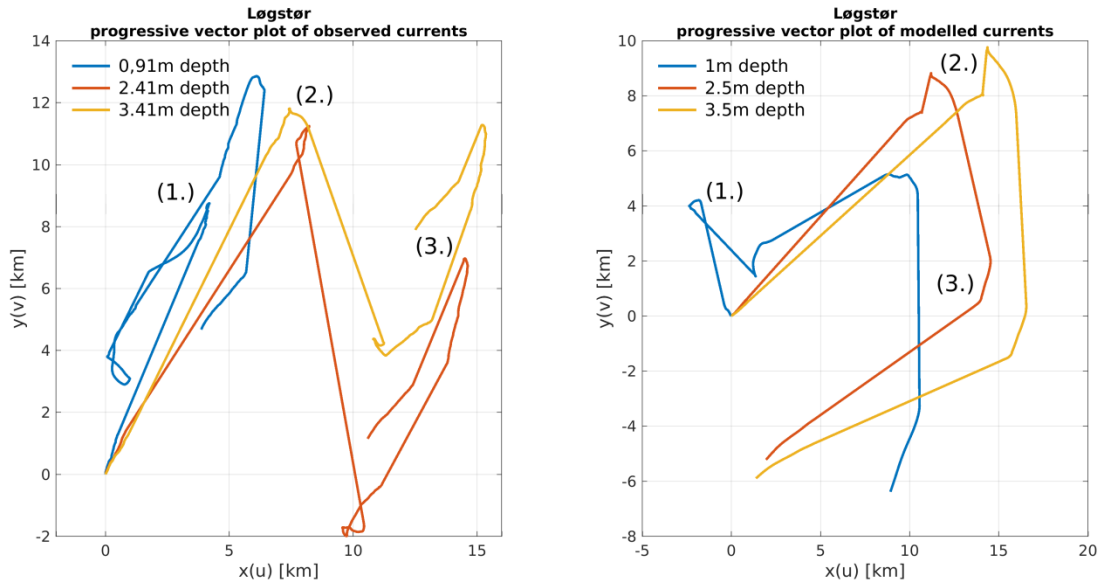

Figure 2.4. comparison of progressive vector plots at 3 depth: measured currents from the campaign in 2017 (left) and modelled currents (right).

2.2 The FLEXSEM framework and applications

Aarhus University has developed the modelling framework FlexSem over the last eight years. FlexSem is a fast, flexible and user-friendly tool targeted explicitly towards scientific and management challenges of the complex biogeochemical processes in coastal ecosystems (Larsen et al. 2017,

2020). FlexSem is a modular marine modelling framework containing a full 3D hydrodynamic (HD) module, a simplified formulation of estuarine hydrodynamics (HDLite), or it can be forced by an external hydrodynamic model. Setups can include complex descriptions of pelagic and benthic biogeochemical processes and dispersal of tracers (e.g. nutrients or particles) or agents (e.g. mussel larvae). FlexSem allows the user to set up computational grids of different complexity ranging from simple box model configurations to high-resolution unstructured grids. It can be applied by non-experts after a short introduction and might therefore be a good candidate to support managers and scientists without the need for extensive computing infrastructure. The code is open source and can, together with the documentation, be downloaded at the FlexSem web page https://marweb.bios.au.dk/Flexsem/.

In the project, the FlexSem framework was further developed to include the Limfjorden at three different spatial resolutions and model complexity:

- Sediment resuspension and plume dispersion model. The 3D sediment resuspension model was a simple physical set-up forced by measured velocities and with a very high spatial resolution of 10 m applied to a smaller area around observed mussel dredging activities. The dispersal and intensity of the sediment plume depended on the amount of resuspension due to mussel dredging activities, the particle sinking velocity and the current speed and direction.

- Ecological model with oxygen depletion for Skive Fjord and Lovns Bredning. The ecological model was a fully 3D coupled hydrodynamic-biogeochemical model extended with new hypoxia development descriptions and a typical spatial resolution of 243 m. The model was used to estimate the positive and negative environmental effects of mussel transplantation before hypoxia events.

- Limfjorden physical model with mussel larvae dispersal. The 3D physical model was a mixed-mesh combining triangles and squares covering an area of 1501.5 km^2 for the whole Limfjorden by 6686 elements with an average horizontal resolution of 474 m (Figure 2.5). An Agent Based Model (ABM) was coupled to the physical model, and individual agents (mussel larvae) were transported around in the 3D model domain to estimate settlement potential and connectivity between areas.

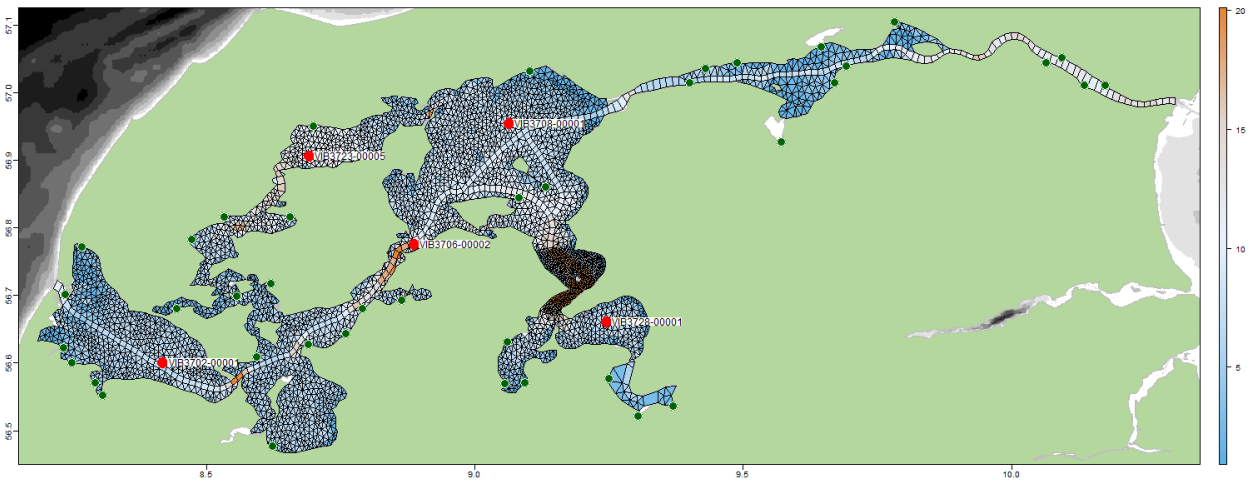

Figure 2.5. FlexSem computational mesh, bathymetry (colour bar), validation stations (red spots) and freshwater sources (green spots).

3. Resuspension and spread of sediment plume after mussel dredging[3]

3.1 Introduction

The EU Common Fishery Policy aims to ensure that fishing is environmental, economically and socially sustainable. Hence, to manage shellfish fisheries, it is important to know the ecological structure and function of the coastal zone and document the impacts of fishing on the ecosystem (Kamermans & Smaal 2002). One of the major concerns of mussel dredging is the resuspension of sediment particles leading to reduced light conditions for seagrasses (Riemann & Hoffmann 1991, Dyekjær et al. 1995, Holmer et al. 2003). Eelgrass (*Zostera marina*) is the most common seagrass species in northern and Western Europe. Light conditions mainly control the depth limit of eelgrass, provided that other losses are constant for the deepest living plants, and is a key indicator under the European Water Framework Directive for the biological quality element 'Macroalgae and angiosperms' (Carstensen et al. 2013). In the Danish Limfjorden, water clarity has not improved despite nutrient reductions of 30% since the 1990'ies and this was attributed to increased resuspension due to mussel removal and declining eelgrass cover (Carstensen et al. 2013). However, the impact of dredging on seagrass ecosystems is complex and far from fully understood, despite various research efforts (Erftemeijer and Lewis 2006). Hence, there is a critical need to improve the ability to make predictions of the extent, severity, and persistence of environmental impacts associated with mussel dredging, especially when conducted close to sensitive habitats such as eelgrass meadows (Erftemeijer and Lewis 2006).

The processes governing the dredge plume generation and transport are complex and depend on many factors, which are often site- and substrate-specific. In the following study, we used the 3D FlexSem model system (Larsen et al. 2017, 2020) as a tool for predicting potential environmental impacts of mussel dredging activities at two study sites in the Limfjorden supported by field data. This study aimed to estimate the effects of mussel dredging on resuspension of sediment particles, i.e. the plume size, intensity, and dispersion in the water column according to recorded dredging events and in different model scenarios. The results will be evaluated and provide input to management plans concerning mussel fishery and the protection of eelgrass beds.

3.2 Field work for model calibration and validation

Field studies were conducted at two different broads of the Limfjorden from the 26th of February to the 4th of March 2017 (Lovns Bredning) and from the 6th to the 10th of March 2017 (Løgstør Bredning). In each sampling area, 16 fixed-position moorings were deployed in two circular sensor arrays around the mussel dredging area (Figure 3.1). The inner array (stations 1 – 8) had a diameter of 200 m, and the outer array (stations 9 – 16) was set up with a diameter of 600 m. Mussel dredging was performed by one fishing boat using four light-Dutch dredges, two on each site of the boat (Eigaard et al., 2011). The trawl starts and end positions were mainly located inside or at the boundary of the inner mooring circle (Figure 3.1). Part of the survey area in Lovns Bredning (including stations 14 and 15) was located inside a small eelgrass protection area (eelgrass box) designated to safeguard resident eelgrass beds from dredging. The dredging process takes a couple of minutes before the collected mussels are rinsed in the water column and taken on board (Figure 3.2). The mussel dredging activities lasted for 1.5 to 2.5 hrs each day, giving 19 and 15 dredge tracks in Lovns Bredning and Løgstør Bredning during the study period. The highest dredging events were 12 in Lovns Bredning and 9 in

3 This work has been published in: Pastor, A., Larsen, J., Mohn, C., Saurel, C., Petersen, J. K., & Maar, M. (2020). Sediment Transport Model Quantifies Plume Length and Light Conditions From Mussel Dredging. Frontiers in Marine Science, 7, [576530]. https://doi.org/10.3389/fmars.2020.576530

Løgstør Bredning, occurring on the second day at both locations. Each dredge covered a distance of approximately 115 m (Lovns) and 150 m (Løgstør) with a trawling speed of 3.2 knots (Lovns) and 2.6 knots (Løgstør), respectively.

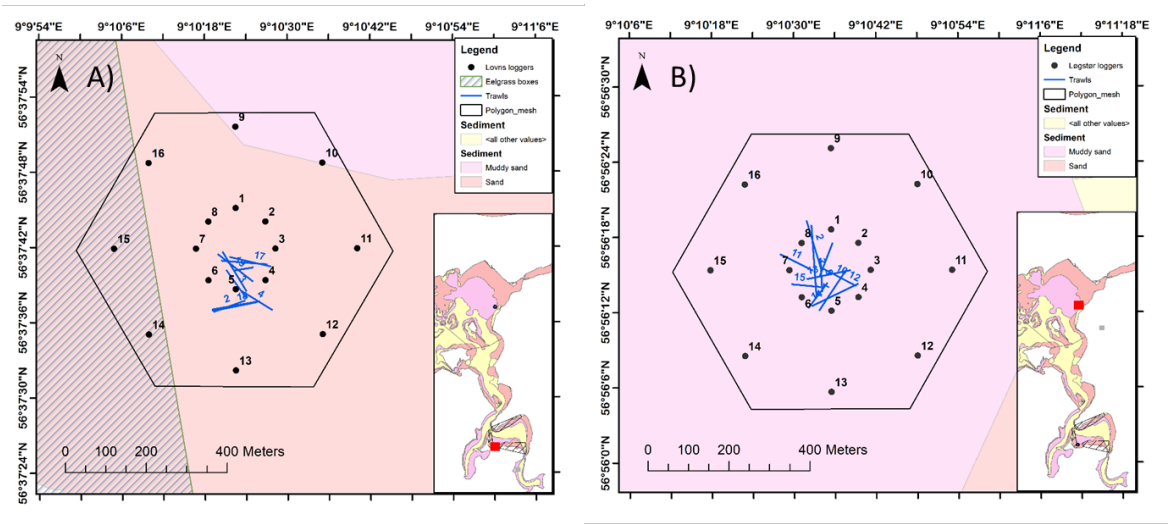

Figure 3.1. Mussel dredging tracks conducted in A) Lovns Bredning and B) Løgstør Bredning. Black circles indicate the loggers' positions (numbered from 1-16). Trawl tracks are blue lines (from 1-19 in Lovns), and the FlexSem model domain are shown as a black polygons (modified from Pastor et al. 2020).

Figure 3.2. Drone image of mussel dredging in Løgstør broad showing next to the left boat the dredge rinsing sediment plume and the small plume along the track of the bottom fishing boat with its dredges deployed. At the bottom of the picture, mussel patches are visible. Photo © DSC DTU Aqua.

Integrated temperature and light loggers (HOBO Pendant Temperature/Light 64K Data Logger) were mounted on each mooring in the two circular arrays at three different water depths (0.5, 1.0 and 3.0 m above seabed). The 48 loggers (3 depths and 16 stations) were deployed in each area over a period of four days, and light intensity time series were collected with a sampling interval of 30 seconds. Five loggers in the Lovns area did not provide any data due to technical problems (two near-surface loggers and three loggers at 1 m above the seabed). However, one bottom logger at Løgstør Bredning failed to provide data. Each time series was filtered using a 3-minute moving average for removing the outliers but retaining sharp changes in light intensity associated with short-lived sediment plumes caused by experimental mussel dredging. Light intensities were min-max normalized by scaling all values in the range 0 to 1 to compensate for significant delicate intensity differences between moorings caused by temporal variability of solar irradiance, spatial heterogeneity in cloud cover and background light attenuation due to the presence of particles other than sedimentary material from mussel dredging. Light intensity anomalies were then calculated at each depth relative to an area-wide average of the min-max normalized data. We used a simple threshold to detect potential evidence for occurrences of dredging related turbid layers in the light logger data. Turbidity signals were detected as when the near-bottom minimum light intensity anomaly (low light events) is smaller than the time-averaged light intensity anomaly at that location minus the highest standard deviation at any location x_n and time step t:

$$min_x\big(\Delta I(x,t)\big) < \overline{\Delta I_t}(x) - max_{(x_n,t)}\big(\sigma_{\Delta I(x_n,t)}\big)$$

where $\Delta I\ (x,t)$ is a time (t) series of light intensity anomalies at a specific location x, $\overline{\Delta I_t}\ (x)$ is the corresponding time-averaged intensity anomaly at location x and $\sigma_{\Delta I(x_n,t)}$ is the standard deviation of intensity anomalies from all mooring locations x_n and time step t (n = number of locations 1 - 16).

An ADCP (600 kHz RDI Workhorse Sentinel) was deployed at each site (station, one at Lovns Bredning mooring, station three at Løgstør Bredning mooring) in a bottom-mounted, upward-looking configuration. 30-second ensembles of 3D velocity components were collected along with corresponding records of beam correlation and error velocity. Each vertical profile had a bin size of 0.5 m, and the first bin was at 1.59 m above the bottom (blanking distance: 0.88 m). The velocity data time series at each bin were filtered using 30 minutes moving average. Only the first six bins contained error-free data (1.59 m to 4.09 m above the bottom). Other depth bins were discarded due to the presence of strong artificial shear layers and noise mainly generated by acoustic signal reflection at the sea surface.

Sediment cores were taken by a diver in the middle of the sampling arrays in Lovns Bredning and at station 3 in Løgstør Bredning using Plexiglas cores. Three replicates were taken on each site and kept in the cold before being processed in the laboratory. The sediment cores had a surface area of 0.0021 m^2, and the sediment column was sectioned into the depth layers: 0-1 cm, 1-2 cm, 2-5 cm and 5-10 cm. Samples from each stratum were homogenized, and subsamples of 10 ml were taken for loss of weight on ignition (LOI) determination. At the same time, the rest of the sediment was used for grain size analysis. Each stratum was then sieved through test sieves of 2mm, 1mm, 500µm, 250µm, 125µm, 63µm. Each fraction was dried at 80ºC until no difference in weight was measured (>48h). The last fraction, <63µm, was filtered onto 47mm pre-dried Whatman GF/C microfiber filters (Sigma-Aldrich Denmark A/S, Copenhagen, Denmark), dried at 80°C for >48 hours in order to determine dry weight. Organic matter was determined for the 10 ml samples for each stratum as LOI at 550°C for 4 hrs (Table 3.1).

3.3 Model development

The FlexSem model system was used to describe the resuspension and transport of different size fractions of sediment particles with varying sinking rates after a dredging event. The computational mesh is made of 4056 equilateral triangles with a characteristic length scale of 10 m, covering a total area of ~ 630 x 630 m. In the vertical, ten layers of 0.5 m thicknesses were used, yielding a total water depth of 5 m. The FlexSem model system was forced by measured time-series of vertical profiles of horizontal current velocities (speed and direction) from the ADCP, assuming the currents to be spatially uniform within the model domain. Thus, the model includes vertical velocity shear, i.e. vertical changes of the horizontal flow, but no explicit vertical velocities. Vertical velocities from the ADCP were at least one order of magnitude smaller than the horizontal currents. The measured vertical profiles were linearly interpolated from the depth bins of the ADCP to the model depth layers.

The area-specific amount of resuspended sediment (kg-DW m^{-2}) was estimated from the measured weight of particles in the sediment (kg-DW m^{-3}) in the surface layer multiplied by the penetration depth of the light Dutch dredge. Since there are no estimates of the depth penetration of the light Dutch dredge, we used the minimum penetration depth of 0.0015 m for the heavy Dutch dredge (Dyekjær et al. 1995). This resulted in a resuspension of 2.6 kg-DW m^{-2} and 4.3 kg-DW m^{-2} in Lovns Bredning and Løgstør Bredning, respectively. The differences were due to a lower amount of sediment in Lovns (17.4 kg m^{-3}) compared to Løgstør (28.3 kg m^{-3}). The approach assumed a 100% efficient resuspension, e.g. that the dredge was in contact with the seafloor at all times. This estimate gave similar or slightly higher results to that of Dyekjær et al. (1995). They found area-specific resuspended sediment of 1.6-2.6 kg-DW m^{-2} from measurements of resuspended matter in the water column before and after dredging using the heavy Dutch-dredge in the Limfjorden (Dyekjær et al. 1995). The total amount of resuspended material (kg-DW) was found by multiplying the area-specific resuspension (kg-DW m^{-2}) by the length (m) of the dredge track (Figure 3.1) and the width of the four dredges (4x1.45 m). The resuspended material was distributed on five particle size fractions (from <0.063 to 1 mm) based on field data obtained from sediment cores. In Lovns Bredning, the dominant particle size was 0.125 to 0.50 mm (fine to medium sand), with concentrations distributed in all five fractions. However, Lovns Bredning also had a higher concentration of the smallest sediment fraction (<0.063 mm, silt) compared to Løgstør Bredning. In Løgstør Bredning, the dominant particles were smaller with 0.063 to 0.25 mm (very fine to fine sand) (Table 3.1).

Settling velocities (V_z) for each sediment size fraction were calculated from the Stokes Law equation. It is based on the assumptions that the flow is highly viscous, the particles are impermeable, and the shapes of particles are spherical (Sun et al., 2016):

$$V_z = \frac{g(p_z - p_w)d^2}{18\,\mu}$$

where g is the gravitational acceleration (m s^2), p_z the density of the settling particle (kg m^{-3}), p_w the density of water (kg m^{-3}), d the diameter of the particle (m), and μ the dynamic viscosity (kg m^{-1} s^{-1}). We assumed that the particles had a density of 2600 kg m^{-3}, i.e. proxy for quartz (Linders et al., 2018). The calculated sinking velocities ranged from 0.002 to 0.53 m s^{-1}. Preliminary model tests showed that the two larger size classes (0.25-1.00 mm) were settling within a few minutes and the three smaller size classes (<0.063-0.25 mm) are the ones that contribute to generate the plume (data not shown). Wind-induced resuspension was not taken into account. The influence of turbulent diffusivity on plume size was tested and only very high turbulence >1E-03 m^2/s resulted in a larger and more diluted plume (Pastor et al. 2020).

3.4 Model scenarios

Model simulations of resuspension of sediment particles to the water column during mussel dredging were first set to reproduce the survey data (Figure 3.1) following the movement of the fishing ship for each day in Lovns Bredning and Løgstør Bredning. The model time-step was set to 1 minute, and the amount of sediment release corresponded to the light-Dutch dredge (see section above). The resuspended sediment was released into the whole water column along the dredge track 3 to 12 times each day, corresponding to the number of dredging activities. Model results provided spatial data on particle concentrations of the different size fraction distributed in the water column over time. At the end of each simulation (1 day), the accumulated sediment concentration settled in the sediment layer within each model element was calculated. The accumulated sediment concentration results are therefore not a representation of the suspended sediment particles at any point in time but are instead a time-independent view of the sediment plume extent. In reality, the actual suspended sediment concentration at any point in time is likely to be lower. The temporal duration of plumes consisting of different size fractions of particles were estimated as an exponential decay of particles over time, where the threshold for plume duration (*PD*) was calculated as $PD = 1/\exp(C_{max})$, where C_{max} is the maximum concentrations of particles in the model domain (i.e. shortly after the release).

Table 3.1. Sediment composition in Lovns Bredning and Løgstør Bredning showing particle size range (mm), sediment class, sediment concentrations (kg m-3) at 0 to 1 cm depth (Lovns) and 0 to 2 cm depth (Løgstør), and representative particle size applied in the estimated sinking rates (Modified from Pastor et al. 2020).

Particle size range (mm)	Sediment class	Sediment concentration (kg m^{-3}) Lovns	Sediment concentration (kg m^{-3}) Løgstør	Representative particle size (mm)	Sinking velocity (m s^{-1})
0.5-1.0	Coarse sand	227	1	1	0.530
0.25-0.5	Medium sand	785	15	0.5	0.132
0.125-0.25	Fine sand	434	2036	0.25	0.033
0.063-0.125	Very fine sand	150	385	0.125	0.008
<0.063	Silt	146	43	0.06	0.002
	Total	1741	2480		

Different model scenarios were also tested in Lovns Bredning (Table 3.2) to analyse the sensitivity of the model to i) amount of suspended sediment, ii) particle size composition, iii) fishing intensity and iv) changes in current speed. Lovns Bredning was chosen due to the proximity of the eelgrass boxes to the trawling activities. In the scenarios, particles were released from one element in the centre of the mesh according to the four dredging events on 28.03.2017 in Lovns Bredning. The mean velocity was 0.05 m s^{-1} during the release. According to Frandsen et al. (2015), a minimum resuspension of 1 kg m^{-2} for the light-Dutch dredge was applied to the first scenario, estimated as the difference in the weight of the gear before and after rinsing immediately after mussel dredging . This value was considered as a minimum estimate because they only considered the sediment collected by the dredge, not including the sediment released during the dredging. The second scenario used the standard release of sediment particles of 2.6 kg m^{-2} in Lovns Bredning (Dyekjær et al. 1995). In the third release scenario, we used a maximum resuspension of 3.7 kg m^{-2} as estimated for Løgstør Bredning. This was considered as a worst-case scenario because the amount of resuspended material was higher than the maximum estimate by Dyekjær et al. (1995) using the heavier Dutch dredge and because it was based on a 100% efficient resuspension. In reality, the dredge jumps over the bottom, scooping up

sediment for a while, then glides over the sea floor without touching the bottom and then collects surface sediment and mussels, creating gaps in the dredge track (Dyekjær et al. 1995). Scenario four used the particle size composition from Løgstør Bredning (Table 3.1). In scenario five, an intense dredging activity was tested with a total of 12 trawls in 1 day. In scenarios six and seven, the simulations started when the maximum and minimum current speeds, observed in the data set. E.g., if the maximum current speed occurred on the 28th of February, the model and the dredging activities were forced to start at that time.

Table 3.2. Model scenarios with description, mean current speed and estimated plume size. The same dredging activities were reproduced in all scenarios based on the four dredging events on 28.02.2017, lasting one minute each. The sediment particles are released from one element in the mesh centre (Modified from Pastor et al. 2020).

Scenario no	Dredging intensity /resuspension	Additional comments	Mean current speed	Plume size
1	4 dredges/ 1.0 kg m^{-2}	Minimum resuspended value	0.05 m s^{-1}	200 m
2	4 dredges/ 2.6 kg m^{-2}	Lovns Bredning	0.05 m s^{-1}	230 m
3	4 dredges/ 3.7 kg m^{-2}	High impact (worst case) scenario with a 0.15 cm penetration in Lovns Bredning	0.05 m s^{-1}	300 m
4	4 dredges/ 2.6 kg m^{-2}	Particle size composition from Løgstør Bredning	0.05 m s^{-1}	175 m
5	12 dredges/ 2.6 kg m^{-2}	Intense dredging	0.05 m s^{-1}	360 m
		Current speeds:		
6	4 dredges/ 2.6 kg m^{-2}	Constant minimum speed	0.02 m s^{-1}	100 m
7	4 dredges/ 2.6 kg m^{-2}	Constant maximum speed	0.15 m s^{-1}	>400 m

3.5 Results

The model estimated the total amount of sediment accumulated on the seabed at the end of the dredging period for each sampling day in Lovns Bredning and Løgstør Bredning. The highest impact was found close to the dredge track due to fast sedimentation of the larger particles, and the signal decreased with distance from the track in the downstream current direction. On the second day at both locations, the highest impact was found corresponding to the highest dredging activity. The smaller particles were transported further away by the prevailing currents, and the impact range varied from 260 m to 540 m in both areas. The impacted area differed between days on the two locations due to differences in current patterns, the number of dredging events and different sediment size fractions at the two locations. Water currents were in general rather uniform over depth without significant vertical shear for most of the sampling period in each area. At the Lovns mooring, the strongest instantaneous currents were directed to the south and west during the first two days of sampling. The highest instantaneous current speeds (0.15 m s^{-1}) were recorded in the bottom-most layers in the early hours of the 2nd of March 2017. At the end of the sampling period (after 2nd March 12:00), currents were considerably weaker (~ 0.02 m s^{-1}) and mainly directed to the south and southeast. At the Løgstør mooring, currents were mainly directed to the northeast with speeds up to 0.10 m s^{-1}, interrupted by short periods of south-westward flow. Instantaneous currents during these flow reversals experienced an episodic amplification of both magnitude and vertical shear. Maximum speeds of up to 0.15 m s^{-1} were recorded in the near-surface layers during the second day (7th March 12:00 – 7th March 18:00).

The model was validated by comparing modelled near-bottom suspended sediment concentrations (g m^{-3}) at the end of each dredging period in Lovns Bredning and Løgstør Bredning with light intensity anomalies measured with the bottom-most light loggers at each mooring. We considered only sampling locations, where the statistical model predicted the presence of potential dredging plumes from light measurements. Modelled sediment concentrations at plume presence locations were inversely related to observed light intensity (Figure 3.3 and 3.4). Modelled occurrences of high sediment concentrations corresponded to negative light intensity anomalies, i.e. stronger light attenuation. This relationship was generally less pronounced in Lovns during the 1st March 2017 sampling campaign (Figure 3.3). Differences between measured light intensity anomalies and model results are likely due to shortcomings in the individual performance of both the numerical and the statistical models. The numerical model only considers sediment introduced by dredging activities and not the background. The statistical presence/absence model might occasionally fail to differentiate correctly between light attenuation caused by dredging plumes and light attenuation caused by natural sediment resuspension events. Consequently, a pronounced mismatch between modelled sediment concentrations and observed light intensity anomalies is expected at locations where plume signals are weak or absent due to low signal-to-noise ratios.

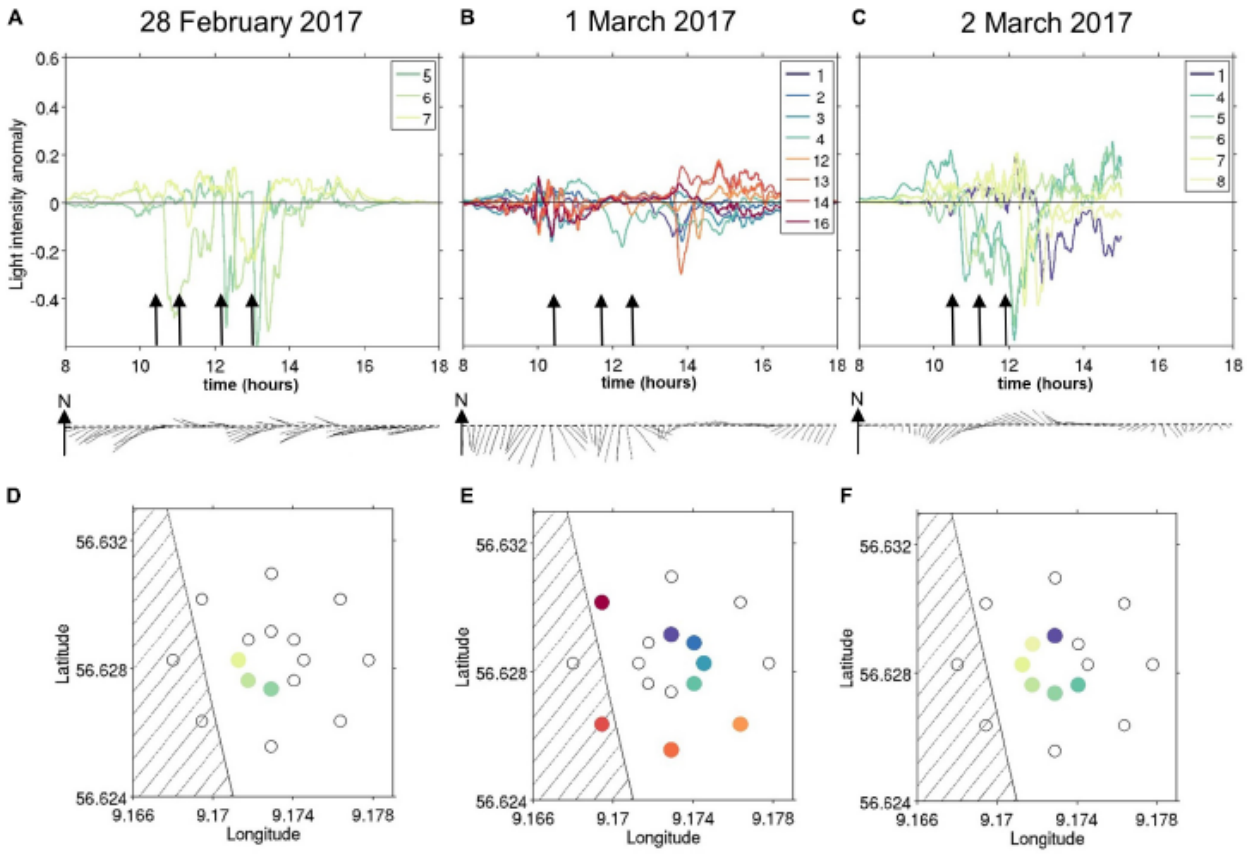

Figure 3.3. Bottom-most (0.5 m) light intensity anomalies from normalized light intensity logger data at all moorings in Lovns Bredning. Time-series during different sampling days are shown in subfigures (A–C) with dredging periods indicated by black arrows. Mooring stations are numbered according to Figure 2A and have different colours. The stick plots below (A–C) display the dominant flow direction in the bottom-most depth layer (see Figure 3 for more information). Stick plots represent both flow magnitude and direction and are equally scaled. In subfigures (D–F), the locations of moorings with detected light intensity anomalies are indicated using the same colour code as in (A–C) for the respective days. The hatched area indicates the location of the eelgrass box.(from Pastor et al. 2020)

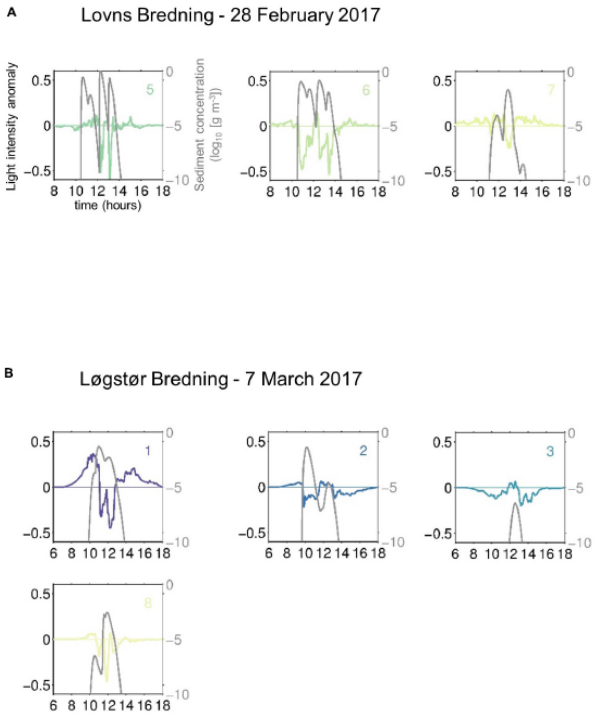

Figure 3.4. Observed time series of light intensity anomalies at plume presence locations (coloured lines, predicted by the detection threshold analysis) versus the modelled sediment concentrations (g m^{-3} on log scale, solid grey lines) at 0.5 m above seabed on the first sampling day at (A) Lovns Bredning and (B) Løgstør Bredning. Coloured lines and numbers refer to predicted stations, as shown in Figure 3.3a. (modified from Pastor et al. 2020).

In the model scenarios, the accumulated sediment on the seabed and the sediment plume length at the end of the dredging period was calculated for Lovns Bredning (Figure 3.5 and Table 4). The plume length was smaller, and the sediment concentrations were lower in scenario one (330 m, Figure 3.5 A) with minimum resuspension compared to the standard scenario two (360 m, Figure 3.5 B). In scenario three, the plume length increased. The sediment concentrations were higher than in scenarios one and two due to the higher amount of resuspended sediment from using the Dutch dredge (>390 m, Figure 3.5 C). In scenario four, the lower proportion of the smallest sediment fraction (<63 mm) with lower sinking rates (Løgstør conditions) resulted in a smaller impact range (310 m) by sedimentation (Figure 3.5 D). With a higher fishing intensity, scenario five showed a larger plume length (450 m) reaching further into the eelgrass box compared to the other scenarios (Figure 3.5E). Scenario six (220 m) showed that low current speeds caused a smaller plume (Figure 3.5F) compared to scenario seven (>390 m) with high current speeds (Figure 3.5 G). The plume intensity varied from 0.62 to 1.79 mg l^{-1} (median) between the tested model scenarios, and the upper quantile showed plume concentrations of 1.22 to 11.61 mg l^{-1}.

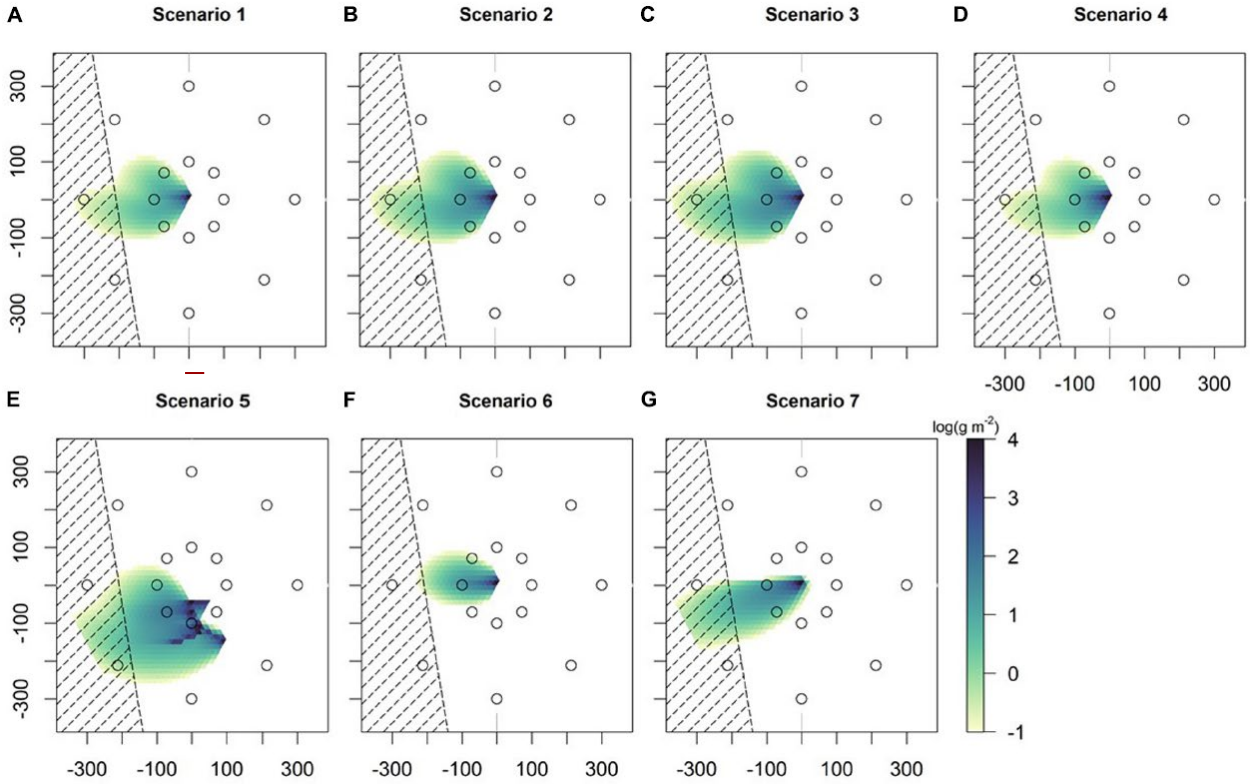

Figure 3.5. Accumulated sediment (g m-2 on log scale) at the end of the trawling activities in Lovns Bredning for the different scenarios (A–G) (nos. 1–7 in Table 3). The hatched area indicates the location of the eelgrass box. Black circles indicate the position of loggers (from Pastor et al. 2020).

3.6 Discussion and conclusions

Quantifying and modelling the transport and fate of sediment released during mussel dredging operations is essential for developing management plans in shallow coastal areas such as the Limfjorden. When used with ecological thresholds, sediment transport and fate modelling form the basis of impact prediction. Here we used the FlexSem model system to calculate the size, duration and intensity of sediment plumes caused by mussel dredging. The distance and direction of the plume were primarily controlled by currents patterns. Currents were relatively uniform without significant vertical shear for most of the sampling period in both areas. The strongest currents were directed to the south and west during the first two days of sampling in Lovns Bredning and mainly to the northeast in Løgstør Bredning. Modelled occurrences of high sediment concentrations corresponded to negative light intensity anomalies in both areas; thus, we recommend this approach for model validation and to make future recommendations on the impact of sediment plumes on light.

The differences in sediment plumes (260 to 540 m) between Lovns Bredning and Løgstør Bredning could be explained by differences in the water current patterns, the sediment particle size composition in the area and the intensity of the trawling defined by the number of dredging activities per day. This last annotation was clearly reflected as the difference between scenario two (four dredging events) and scenario five (12 dredging events) (Figure 3.5). The plume extent was generally 220 to 450 m long at different current speeds and fishing intensities and exceeded 390 m at the most extreme event of constant, high current speed (0.15 m s^{-1}) in the scenarios. The plume duration was estimated to be approximately one hour for the smallest size fraction (<0.063 mm, silt). Non-cohesive sediment has previously been shown to settle within the first 30-60 min (Riemann & Hoffmann 1991). From the five

sediment fractions used in the model, only the smallest fractions (0.063-0.125 and <0.063 mm) contributed to the plume and remained in the water column for a longer period. The rest of the particles sank within the first minutes after the resuspension occurred.

Light attenuation in the Limfjorden mainly depends on suspended inorganic matter, and less on chlorophyll a concentrations and is closely related to wind-induced resuspension (Dyekjær et al., 1995; Olesen, 1996). The model showed that the median concentration of the sediment plume from the dredging events (0.62–1.79 mg l^{-1}) was slightly lower than measured background median values of 2.9 mg l^{-1} in the Limfjorden (Olesen, 1996). On the other hand, the 75%-percentiles values showed similar values (1.22–11.61 mg l^{-1}) to the upper quantile of 4.7 mg l^{-1} of measurements (Olesen, 1996). The mussel fishery season starts in September and ends in June the following year, after which it closes for two consecutive months. The eelgrass growth season is from May to October (Eriander, 2017), with maximum biomass production during the summer months (Boström et al., 2014). Hence, there will be a short seasonal overlap from April to June and between September and October, but not during the summer period with maximum eelgrass growth.

The recorded fishery activity in Lovns Bredning is variable from year to year. In 2017, 28 boat events of fishing activity (the same boat can fish several times over a period of time) were distributed on 13 days from April to October. However, in 2018, there were 64 boat events for 17 fishing days (Danish Fisheries Agency). Hence, the daily fishing impact corresponded to 6–8% of the eelgrass growth season. Around 27 and 40% (in 2017 and 2018, respectively) of the fishing took place less than 500 m away from the eelgrass box. This was due to the nearby high standing stock of mussel seeds in the area. The eelgrass box contains a buffer zone of 300 m around the eelgrass. Hence, if fishing is occurring close to the box, the plume may reach the eelgrass when there is high current speed events or/and intense fishing. Nevertheless, the impact will probably be minor at the given fishing frequency in Lovns Bredning. In Løgstør Bredning, the daily fishing activity was higher than for Lovns Bredning with 16–35% of the growing season in 2017 and 2018, respectively (126–322 boat events, 33– 75 days), whereas only <1% of the fishing occurred less than 500 m from the eelgrass box. On average, <2 and 1.2% of Lovns and Løgstør areas, respectively, are impacted by direct dredging effects from April to October in 2017. Hence, although there are more fishing days in Løgstør than in Lovns, the fishery in Løgstør is spread over a larger area further away from the coastline and the eelgrass habitats. Moreover, in all Natura 2000 areas, the eelgrass boxes take into consideration all the eelgrass beds established and the potential habitat that could be colonized by eelgrass. Overall, for the two basins, the estimated indirect effects from fishing on light conditions and eelgrass growth must be considered of minor importance as long as the daily fishing intensity is kept at the same low level.

Compared to hydrodynamic and wave modelling, sediment transport modelling has many challenges due to the more complex nature of sediment transport processes and lack of data, which is a considerable obstacle to improving model predictions. The key physical processes that control the extent, intensity and duration of sediment plumes from dredging are very complex and present many challenges in model calibration and validation. For example, mussel dredging and wind-generated resuspension fall within the same temporal magnitude (Dyekjær et al., 1995). The present model does not account for wind or other events that generate multiple resuspension events before, during and after the dredging. It is also important to consider that once a trawling event resuspends the sediment of an area, it becomes easily resuspended with a second trawl happening nearby or by a wind event. This will cause multiple unaccounted resuspension events in addition to the ones already modelled. Natural turbidity events are common in shallow environments. Although unidirectional currents may influence resuspension and transport of suspended material, wind-driven waves might be the primary mechanism of turbidity generation. In addition, parameter values used in sediment transport models are often not reported in Environmental Impact Assessment (EIA) documentation, leaving considerable uncertainty in assessing the model performance and inter-comparison with other models.

Sediment transport models are often not calibrated or validated due to the lack of relevant field data. The approach presented here, including model-data comparisons, is a significant step forward within this field. They should be combined as part of the monitoring efforts and incorporated into EIAs regularly to allow model validation and a deeper understanding of the sediment dynamics. Currently, sediment transport modelling does not include ambient sediments. Although conceptually there are potential benefits from including ambient sediments, in practice, the issue of ambient sediment modelling needs to be carefully assessed in the future because it requires more data and poses several technical challenges.

Improving model accuracy should be considered in the context of current science and financial costs. For example, settling velocity is essential for the dredge plume modelling, and measuring the settling velocity of particles in the dredge plume can be done using existing technologies. On the other hand, cohesive sediment resuspension under surface wave forcing appears to be poorly understood and not well represented in sediment transport models. Future studies would be optimal to start recording field data on sedimentation before the dredging operations start (also known as the continuous approach). This was attempted in the study but would require many more stations along several transects, and it does not prove easy to be close enough to the fishing area due to the length of the wires and tracks. A successful design could allow us to understand the dynamics in the initial phases and estimate how other effects such as wind account for resuspension since we can be potentially under-estimating suspended sediment concentrations. No acceptable threshold levels of sedimentation rate are known for eelgrass, and it would be essential to determine which levels of resuspended sediment are detrimental to eelgrass growth.

4. Mussel transplantation to mitigate hypoxia[4]

4.1 Introduction

Mass mortality of blue mussels occurs every summer in the hypoxic, stratified parts of Danish estuaries, and the oxygen consumption of decaying mussels is suspected to accelerate the hypoxia. Dead mussel tissue is of high food quality to bacteria degrades faster than older, less labile detritus in the system (Lomstein et al. 2006). Following a mass mortality event, the degradation of mussel tissue will increase oxygen consumption and sediment nutrient fluxes, which may elevate Chl *a* concentration in the system and affect the water quality negatively (Lomstein et al. 2006). Hence, mussel fishery before hypoxia could positively affect eutrophic environments such as Lovns Bredning by reducing mass mortalities of mussels and the associated adverse effects on water quality (Dolmer & Frandsen 2002). This could be a solution to mitigate hypoxia as long as the ecological condition is bad in the area, whereas the overall aim is to improve the health of the ecosystem through nutrient load reductions. On the other hand, mussel dredging can have a short-term negative environmental impact due to the resuspension of sediment particles affecting the water clarity, increased sediment oxygen consumption, and nutrient release (Riemann & Hoffmann 1991, Dyekjær et al. 1995, Holmer et al. 2003). Mussels are also important filter-feeders and deplete phytoplankton in the water column (Asmus & Asmus 1991, Nielsen & Maar 2007, Petersen et al. 2013). Removal of mussels in large quantities may reduce the system's filtration capacity, leading to increased phytoplankton biomass and sedimentation. Hence, the overall effects on the ecosystem due to mussel transplantation is difficult to predict due to the different, in some cases counteracting, eco-physiological processes combined with the physical transport of oxygen (vertical mixing, advection and atmospheric exchange). In this case, 3D ecosystem modelling is a valuable tool to evaluate the overall outcome of different management scenarios of mussel fishing.

The study aimed to investigate if mussel transplantation from areas frequently exposed to hypoxia could deaccelerate the hypoxia event in the donor area and potentially be used as a mitigation tool for management. The objectives were to i) estimate the oxygen consumption due to degradation of dead mussel tissue, ii) measure changes in bottom oxygen during dredging, iii) conduct different scenarios of mussel removal and its effects on hypoxia using a 3D ecological model and iv) evaluate the potential of using mussel transplantation for hypoxia mitigation in the management of coastal ‘problem’ areas.

4.2 Laboratory work

The oxygen consumption of decaying blue mussels (*Mytilus edulis*) was estimated and used to parameterize the model. Mussels were collected from a mussel longline farm in Limfjorden in June 2018 and transported to the nearby Danish Shellfish Centre laboratory facilities. Mussel shell length varied between 22 and 28 mm, and the flesh wet weight (*FWWt*) between 0.2 and 0.6 g. Prior to the respiration experiment, live mussels were placed in a sealed container with 0.5 mm height of seawater and left under the sun for less than 24h. Shell was removed from the dead mussels, and the whole weighed flesh was placed into a 144 ml respiration chamber filled with UV treated and filtered seawater (0.2 µm). A magnet stirrer placed in the respiration chamber ensured constant stirring while coupled to an outside rotating magnet. The oxygen concentration was measured using fibre-optic oxygen sensor held next to oxygen sensor spots present in the respiration chamber (OXY-4 Loligo Sys-

[4] This work has been published as: Maar, M., Larsen, J., Saurel, C., Mohn, C., Murawski, J., & Petersen, J. K. (2021). Mussel transplantation as a tool to mitigate hypoxia in eutrophic areas. Hydrobiologia, 848, 1553-1573. https://doi.org/10.1007/s10750-021-04545-6

tem ApS, Tjele, Denmark). The constant temperature was maintained in the respiration chambers using a temperature-regulated bath (TMP-REG instrument - Pt100 probe, Loligo System ApS, Tjele, Denmark). The decreasing dissolved oxygen concentration was continuously monitored until no more oxygen was present in the chamber under three temperature treatments: 15, 20 and 25°C. Treatments were run separately using four respiration chambers simultaneously. One chamber was used as a control with no mussels, and the three remaining contained each an individual mussel without the shell. Each treatment experiment was repeated at least once. Overall consumption rate and maximum rate were calculated for each decaying mussels taking into consideration temperature, salinity and pressure. The duration of each experiment varied between 30 minutes and nine hour, depending on the temperature. The overall oxygen consumption rate, *DR*, for the decaying mussel (mg-O_2 g-C^{-1} day^{-1}) was calculated as:

$$DR = \frac{[O_{2(f)}]-[O_{2(i)}]}{(T_f - T_i)} \times \frac{V}{(FWWt \times CC)} \quad (1)$$

where $[O_{2(f)}]$ and $[O_{2(i)}]$ are the final and initial oxygen concentration, respectively, in mg L^{-1}, T_f and T_i the time at the end and beginning of the experiment in days, *FWWt* (g), *V* is the volume (l) of the chamber, and *CC* the conversion factor from *FWWt* to carbon, *CC* = 0.1 g-C g-*FWWt* $^{-1}$ (Saraiva et al. 2011). The maximum consumption rate was calculated as above using the initial percentage air saturation at 20% and final percentage air saturation at 5% in the respiration chamber. The degradation rate (mmol-C mmol-C^{-1} d^{-1}) of mussel tissue was estimated from the oxygen consumption rate using a mol-O_2 mol-C^{-1} ratio of 1 and the mol weights of carbon (12 g mol^{-1}) and oxygen (32 g mol^{-1}). The temperature coefficient Q_{10} value was estimated as:

$$Q_{10} = \left(\frac{R2}{R1}\right)^{\left(\frac{10}{T2-T1}\right)} \quad (2)$$

using the estimated rates *R1* and *R2* at the corresponding temperature *T1*=15°C and *T2*=25°C, respectively.

4.3 Field study

The aim of the field work was to measure changes in oxygen concentrations in bottom water due to the resuspension of oxygen-consuming particles during mussel dredging. Field studies were conducted from 28th of February to 1st of March 2017 in Lovns Bredning and from 7 – 9th of March 2017 in Løgstør Bredning (Figure 1A). Mussel dredging by one fishing boat using four light dredges took place inside a mooring circle and consisted of three to 12 tracks for approximately two hours each day. Each dredge lasted a few minutes and covered a distance of roughly between 115 m and 150 m, with a trawling speed of 3.2 and 2.6 knots in Lovns Bredning and Løgstør Bredning, respectively. Water column depth was 5.2 and 6.3 m in Lovns Bredning and Løgstør Bredning, respectively.

In each sampling area, four fixed-position moorings were deployed in a circular sensor array with a diameter of 200 m with the locations 'North' (station 1), 'East' (station 3), 'South' (station 5) and 'West' (station 7) (Figure 4.1B). Salinity loggers (HOBO 64k Data logger) and oxygen loggers (PME miniDOT dissolved oxygen logger) were mounted on each mooring at a water depth 0.5 m above the seabed. For each time series, linear correlation analysis was applied to estimate the change in oxygen consumption using a significance level of $p<0.05$. Bottom salinity was analysed to ensure that measurements were conducted in the same water mass at each station. Current velocity and direction were estimated by a 600 kHz RDI Workhorse Sentinel deployed at each site (station 1 at Lovns Bredning and station 3 at Løgstør Bredning) in a bottom-mounted, upward-looking configuration designed to measure 30-second ensembles of 3D velocity components.

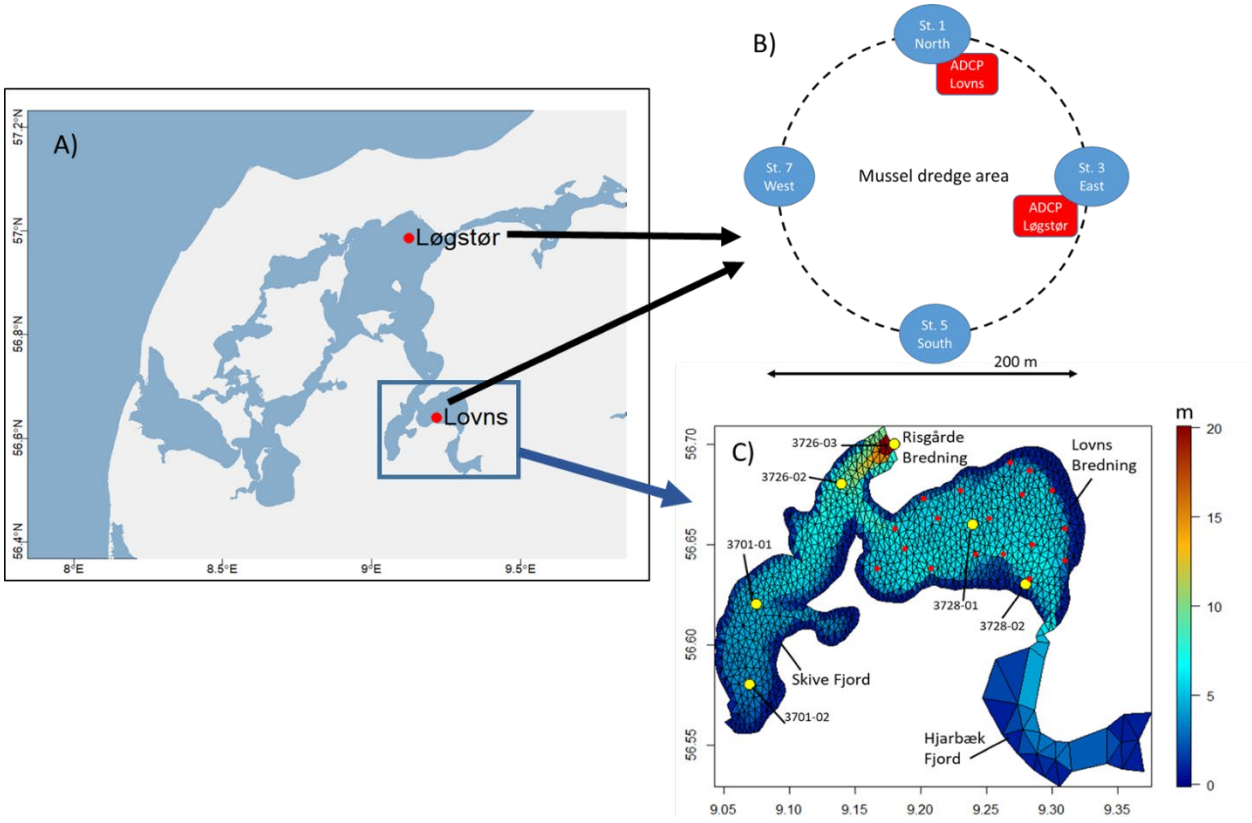

Figure 4.1. A) Map of the Limfjorden showing sampling sites (red) for mussel dredging and oxygen measurements and the model domain (blue box). B) Field sampling in mussel dredging area showing the position of the four stations with loggers and the ADCP. C) The bathymetry (m) and mesh (polygons) of the model domain for Skive Fjord and Lovns Bredning. The monitoring stations of pelagic variables are shown as yellow spots and the mussel biomass sampling locations as red spots. Station 3726-03 is located at the open model boundary to Risgårde Bredning. From Maar et al. 2021.

4.4 Model set-up and scenarios

4.4.1 Model set-up

The model area is Skive Fjord and Lovns Bredning, located in the inner part of the Limfjorden with salinities from 15 to 27 (Figure 4.1A). Lovns Bredning is connected to Hjarbæk Fjord by an open sluice in the south-eastern part, where the salinity varies from 6 to 12. Skive Fjord is connected to Risgårde Bredning at the northern open boundary. Skive Fjord and Lovns Bredning are strongly stratified and highly eutrophic, with intense hypoxia (<2 mg l^{-1}) occurring every summer. Mussel fishing is allowed in Skive Fjord and Lovns Bredning at water depths >2 m and outside the protected 'eelgrass boxes', but not in Hjarbæk Fjord. The biogeochemical model DANECO was coupled to a 3D hydrodynamic model in the FlexSem framework (Larsen et al. 2017) using an unstructured computational mesh (1939 elements) with an average and maximum horizontal resolution of 243 m and 1952 m, respectively (Figure 4.1C). Open boundary data of physical (temperature and salinity) and biogeochemical state variables were obtained from the monitoring station (https://oda.dk) in Løgstør Bredning (the adjacent basin) combined with extra research data from the boundary area for the years 2010-2011 (Timmermann et al. 2019). Open boundary data of current velocities and water level were obtained from a previous model run of the Limfjorden model using the 3D ocean circulation HBM. River discharges of freshwater, inorganic nutrients (NO_3, NH_4, PO_4) and detritus (C, N, P) from six sources

were obtained from the catchment model SWAT applied to the Limfjorden (Molina-Navarro et al. 2017, Thodsen et al. 2018).

4.4.2 DANECO biogeochemical model

The DANECO model further develops the Microplankton-Detritus model by Tett (1998) adapted to Danish fjord systems (Maar et al. 2010, Timmermann et al. 2010). DANECO describes benthic and pelagic biogeochemical cycles of carbon, nitrogen and phosphorus through microplankton (auto- and heterotrophs), detritus and mesozooplankton biomass associated changes in dissolved concentrations of nitrate, ammonium, phosphate and oxygen and adsorbed phosphate to mineral particles (Figure 4.2). Separate state variables for C, N and P in biomass and detritus are applied, allowing for varying C:N:P ratios in organic particles. Chl *a* concentrations are derived from the internal N-content of phytoplankton cells using a conversion factor of 2.0 mg Chl *a* mmol-N^{-1}. The pelagic system is two-way coupled to a biogeochemical sediment model through sedimentation and resuspension of organic matter and diffusive fluxes of nutrients and oxygen (Petersen et al. 2017, Maar et al. 2018). Sedimenting detritus enters the unconsolidated top layer in the sediment. It is gradually respired and re-mineralised by bacteria, transferred to the consolidated sediment by deposit feeders or resuspended to the water column (Figure 4.2). Dissolved inorganic nutrients and oxygen are transferred between the sediment pore water and pelagic compartment by diffusive fluxes. A fraction of the recycled NH_4 is lost in a coupled nitrification-denitrification process. Under oxidizing conditions, PO_4 is retained in the sediment by adsorption to Fe or Mn and released when the sediment becomes reduced (anoxic). Benthic suspension feeders (i.e. blue mussels) ingest microplankton in the bottom water, whereas deposit feeders ingest detritus in the sediment. Mussel ingestion ceases at very low and high Chl *a* concentrations (<0.5 mg Chl *a* m^{-3} and >20 mg Chl *a* m^{-3}, respectively). The ingested matter by benthos is recycled into inorganic nutrients through respiration and excretion or into detritus through defecation and death. Dead mussels were degraded over time using the measured temperature-dependent rate (see the previous section). Suspension feeders were set to be more resistant to hypoxia compared to the more sensitive deposit feeders. Predation mortality was included on both benthos groups, where starfish are the main consumer of blue mussels.

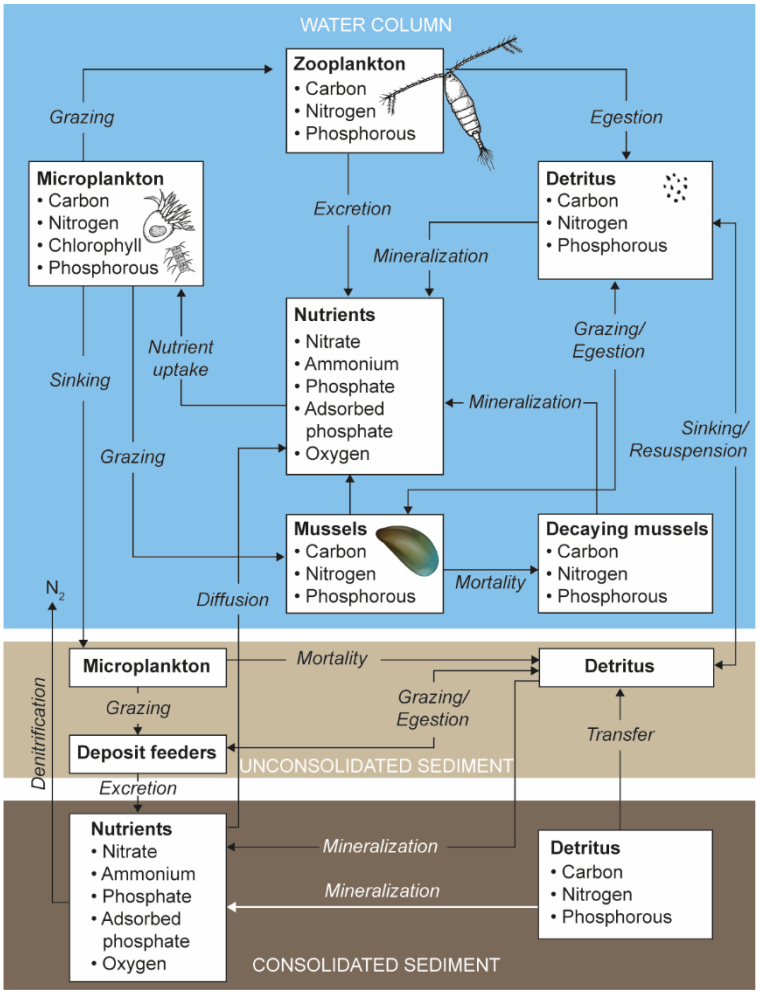

Figure 4.2. Diagram of the DANECO model. The model describes processes (arrows) in the water column, the unconsolidated sediment with resuspension and the consolidated sediment. Boxes show state variables of biomass and detritus compartments with varying internal nutrients-ratios and inorganic nutrients (From Maar et al. 2021).

Fishing of blue mussels was based on recorded landings (wet weight of the whole mussel with shell, *WW*) from the area. It took place on mussel beds with densities >1 kg-WW m^{-2} at water depth >2 m during periods without hypoxia (>4 mg-O_2 l^{-1}) according to the fishing regulations (Christoffersen et al. 2012). For resuspension effects due to dredging, we assumed a resuspension of 0.40 kg-sediment (kg of fished mussels) $^{-1}$ using the light Dutch dredge (Eigaard et al. 2011). Resuspension of oxygen-consuming substances (e.g. H_2S) from the sediment to the overlying water column was not explicitly described by the model. Instead, an oxygen consumption corresponding to 62 mg-O_2 (kg-WW of fished mussels)$^{-1}$ h^{-1} was added to the bottom layer of the model based on laboratory experiments with sediment cores from the Limfjorden (Dyekjær et al. 1995). For pore water nutrients and organic matter in the sediment, we assumed that a fixed fraction in the model was resuspended per kg of fished mussels obtained from model calibration against previous measurements. Hence, the amount of resuspended material varied in time and space depending on the sediment concentrations. The model was calibrated for the year 2010 and validated for the year 2011 using monitoring data from station 3727-01 in Skive Fjord (Figure 1C) with the most comprehensive data of biogeochemical variables in the study area. The model was further validated for bottom oxygen measured with a CTD mounted oxygen probe at five stations in Skive Fjord and Lovns Bredning

4.4.3 Model scenarios

The reference run (REF) for the year 2011 used the reported annual fishing intensity distributed evenly over the ten fishing months (hence not during summer closing). The fished mussels were 1800 t-WW in Lovns Bredning and 2350 t-WW in Skive Fjord in 2011 (Christoffersen et al. 2012). The actual fishery was lower than the total allowable catch (7000 t-WW) in 2011 due to the hypoxia events. We applied the same fishing in the scenarios in the reference run plus mussel transplantation in Lovns Bredning. The fishermen can work at least three days in scenario one (SCE1) and a maximum of five days in scenario two (SCE2) per week. The fishing boats can catch and relay up to 300 t-WW per day, corresponding to a weekly amount of 900 t-WW and 1500 t-WW in scenario one and two, respectively. We assumed that mussel transplants were taking place in the last week of May and first three weeks of June (calendar days 142-167) before the hypoxia events start. Hence, total mussel transplantation was 3600 and 6000 t-WW in scenario 1 and 2, respectively, during a four-week period (Table 1). The transplanted biomass corresponded to 4% and 6% of the total mussel biomass in scenario one and two, respectively. This type of fishery is more intense than normal fishery for human consumption, which is distributed over 10 months. Fishing was restricted to areas in the model with mussel densities >1.0 kg-WW m^{-2} and water depths >2 m. The removed mussel biomass was converted to nitrogen using 1.5% N t-WW^{-1} (Nielsen et al. 2016).

4.5 Results

4.5.1 Laboratory and field experiments

The average (±SD) degradation rate of dead mussel tissue measured in the laboratory experiments was 0.084±0.018 mmol-C mmol-C^{-1} d^{-1} at 15°C, and the estimated temperature coefficient (Q_{10}) was 2.0 (Figure 4.3). The estimated values were used to parameterize the oxygen consumption during the degradation of dead mussels in the DANECO model.

In Løgstør Bredning, with the highest fishing intensity, there was a significant oxygen decrease at all stations located in the downstream current direction from dredging on all three days. One exception is station South, on 9 March, which was located opposite to the main current direction, but here dredging took place very close to the station. The strongest signal (-0.23 mg-O_2 l^{-1} h^{-1}) was found on the 8th of March, with the highest mussel dredging activity. In Lovns Bredning, with less fishing, there was no significant decrease in oxygen concentrations in any direction during the two days of mussel dredging.

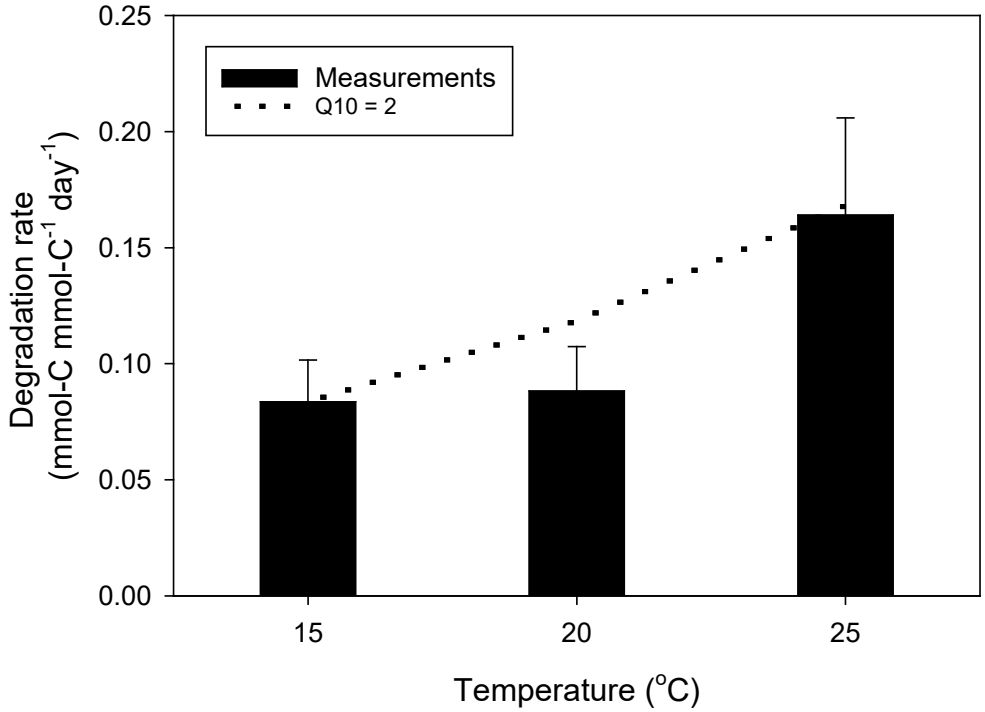

Figure 4.3. Average (± SD) degradation rates (mmol-C mmol-C^{-1}day^{-1}) of dead mussel flesh at temperatures 15ºC, 20ºC and25ºC from experiments and the line shows Q10 = 2.0 (Modified from Maar et al. 2021).

4.5.2 Model results

Model performance of ecological variables for Skive Fjord (the validation year 2011) was all either good or reasonable according to the metrics plots except for bottom Chl *a* concentrations, which showed a low seasonal correlation with observations due to an offset during the spring bloom. The scenario with the highest effort of mussel transplantation, SCE2, always showed higher responses of ecological variables than SCE1 (less fishing) when compared to REF, but the overall patterns compared to REF were similar. Mussels were mainly transplanted from water depths between two and five meters with the highest mussel biomass and, to a lesser extent from five to seven meters in Lovns Bredning (Figure 4.4A). The reference bottom oxygen concentrations showed the lowest values (<0.2 mg l^{-1}) from 4 to 7 m depth during summer and increased almost linearly towards the coast with up to 4.9 mg l^{-1} (Figure 4.4B). Both scenarios showed that bottom oxygen concentrations increased shortly after the mussel transplantation and mainly in the depth interval 3-5 m with 0.2-0.4 mg l^{-1} (16-56%) in Lovns Bredning (Figure 4.4B). The maximum local spatial increase was 0.6 mg l$^{-1,}$ and there were only minor changes outside Lovns Bredning. On basin scale (>2 m depth), the oxygen increase corresponded to 8.6% in SCE2. Hence, bottom oxygen was most improved in the areas with the highest mussel fishery in Lovns Bredning. In contrast, the deeper areas (>5 m) with lower mussel fishery and lower oxygen levels were unaffected. Mussel biomass first decreased over time due to removal by fishing in SCE1 and SCE2 but soon recovered and even exceeded the biomass in REF from August and onwards. The higher survival of mussels mainly occurred in the depth range between three and five meters, with up to 28% more mussels in SCE2 (Figure 4.4C). Spatially, the maximum increase was 200% at the mussel beds located in the eastern part. There were an average of 8% and 14% more mussels on the basin scale in August at >2 m depth in SCE1 and SCE2, respectively. Likewise, mussel ingestion was lower than REF in the beginning but increased to higher levels from around July.

Bottom DIN- and phosphate concentrations showed no changes during mussel transplantation but then decreased with up to 2.2 mmol-DIN m^{-3} and 0.22 mmol-PO_4 m^{-3} in SCE2 from mid-June and onwards due to better oxygen conditions and higher survival of mussels. Surface Chl *a* concentrations generally followed the same pattern as for nutrients and decreased with up to 1.2 mg m^{-3} interrupted by occasional mixing events. The highest changes in surface Chl *a* concentrations were found at >4 m depth (Figure 4.5). The neighbouring basins, Skive and Hjarbæk Fjord, also showed improvements in Chl *a* concentrations. Secchi depths first decreased with up to 0.02 m due to increased resuspension from fishing but then improved with up to 0.08 m during July - August. On basin scale (>2 m depth), DIN- and PO4 concentrations decreased 4.7% and 5.3%, respectively, Chl *a* concentrations decreased 4.2%, and Secchi depth increased 1.7% in SCE2.

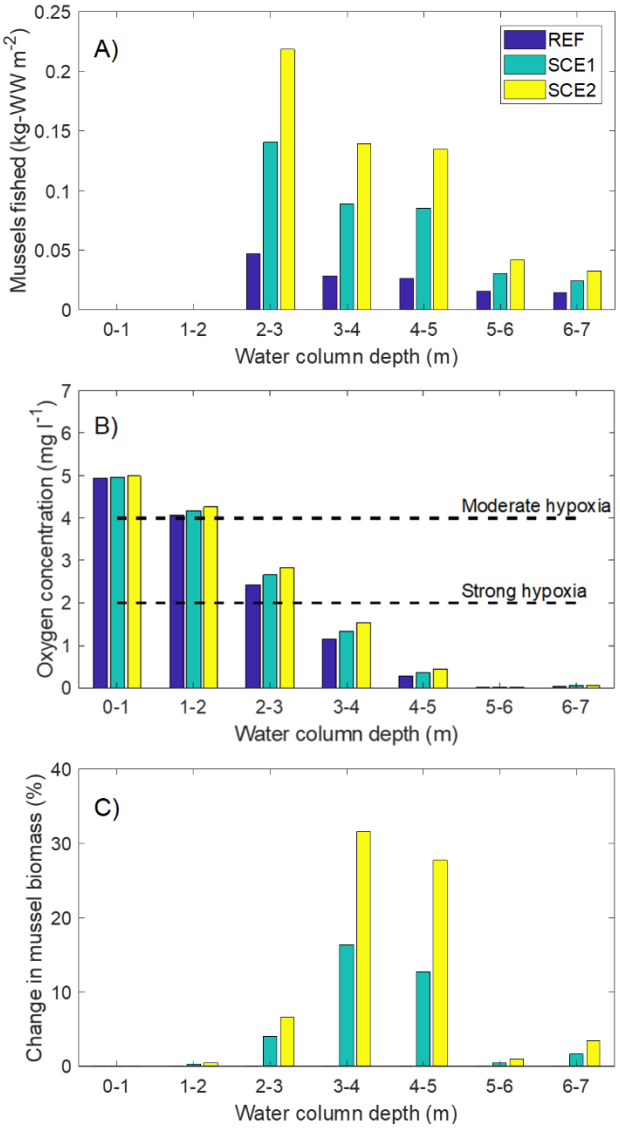

Figure 4.4. A) Annual amount of fished and transplanted mussels (kg-WW m^{-2}), B) minimum bottom oxygen concentration (mg-O_2 l^{-1}) from mid-June to July averaged for 1 m water depths intervals in Lovns Bredning and C) the %-change in mussel biomass in August in scenarios relative to REF. The dotted lines indicate the thresholds for strong hypoxia (<2 mg l^{-1}) and moderate hypoxia (2-4 mg l^{-1}). Modified from Maar et al. 2021.

4.6 Discussion and conclusion

Intense mussel transplantation during May-June on a system with bad ecological conditions showed positive effects on the ecosystem the following summer months in better oxygen conditions, higher survival of mussels, lower nutrient- and Chl *a* concentration and higher Secchi depths. The highest survival of mussels was found at between two and five meters depth, where there was an increase in oxygen concentrations from 0.2 to 0.4 mg l^{-1} weakening the hypoxic condition (Figure 4.4). Hence, the modelled mitigation showed the highest effect at intermediate depths with strong hypoxia and high mussel densities and not in the deeper, stratified parts with fewer mussels. The highest changes in surface Chl *a* concentrations were found at >4 m depth for a larger area (Figure 4.5). The relative reduction of Chl *a* concentration was 4.2% on basin-scale in SCE2 with 90 t-N removed by mussel transplantation. Hence, the mussel transplantation showed similar environmental effects in the short term (<1 year) as mussel mitigation cultures (3.3%) (Timmermann et al. 2019). The marine measures using mussels were more effective than land-based nutrient reductions (0.5%), probably due to high nutrient immobilization by mussels and a lag-time in achieving steady-state conditions at lower land-based nutrient inputs (Timmermann et al. 2019). In the receiver area for mussel transplantation, the filtration of particles by the transplanted mussels also has the potential to improve water clarity and reduce Chl *a* concentrations (Møhlenberg 1995, Nielsen & Maar 2007). These effects will depend on the local environmental conditions and the survival and growth of the mussels but were not further investigated in the present study. It should also be emphasized that the intense dredging activities can lead to immediate, short-term negative effects (e.g. decrease in oxygen and Secchi depths) on the system and should only be applied in areas with frequent hypoxia-related mass mortalities of mussels. The present modelling exercise helped to identify optimal water depths for fishing and the spatial-temporal environmental impact of mussel transplantation concerning hypoxia mitigation, which can be used in the annual fishing plans of the area. In conclusion, the transplantation of mussel biomass (otherwise lost from the system) can be considered as a management tool to improve the water quality of eutrophic ecosystems with frequent hypoxia.

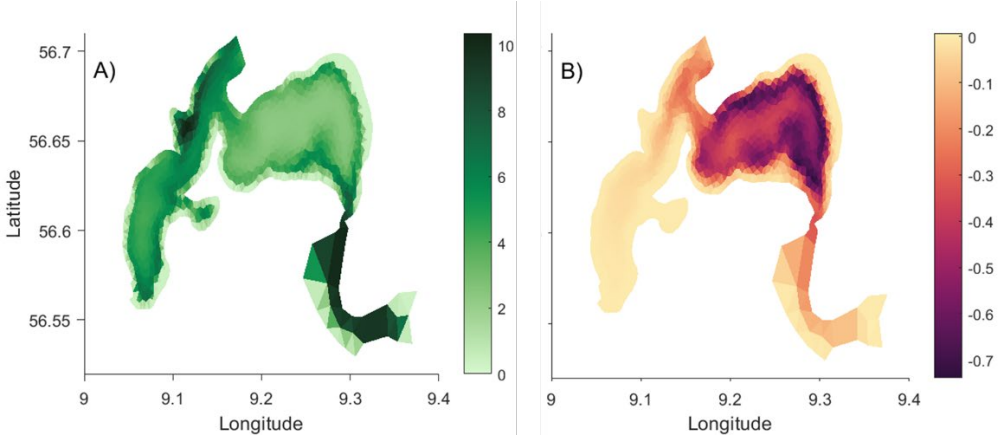

Figure 4.5. A) Average surface Chl a concentrations (mg m^{-3}) and B) average changes in surface Chl a concentrations (mg m^{-3}) in SCE2 from mid-June to July (Modified from Maar et al. 2021).

5. Mussel larvae dispersal and effects of fishery on mussel recruitment

5.1 Introduction

The Limfjorden mussel fishery targets large mussel beds of commercial size (mussel shell length >45 mm) and wild seeds for mussel relaying and bottom culture (mussel shell length < 45 mm). Mussel fishermen are known to come back to previously fished beds. With the use of “black box” (BB) system designed to survey the mussel fishery in Denmark (Danish AgriFish Agency, 2016), it has been possible to compare fishing patterns in the Limfjorden (Figure 5.1). The BB records date, time, position, speed of course and fishing activities such as winch rotation every 10s (Nielsen et al. 2021). Most of the mussel beds in the Limfjorden are being fished either in several consecutive years, or every two to three years (Figure 5.1), indicating that there is mussel recruitment in fished beds. It has thus been hypothesised that mussel fishing could have a positive impact of increasing the mussel recruitment by thinning the mussel beds, which is the action of extracting some of the mussel biomass of the mussel bed by fishing. Thinning could reduce 1) intraspecific competition for food; 2) intraspecific competition for space for the larvae to settle; and 3) the potential predation of young larvae by the cannibalistic behaviour with filtering adult mussels (Porri et al 2008; André et al., 1933; Foret 2018).

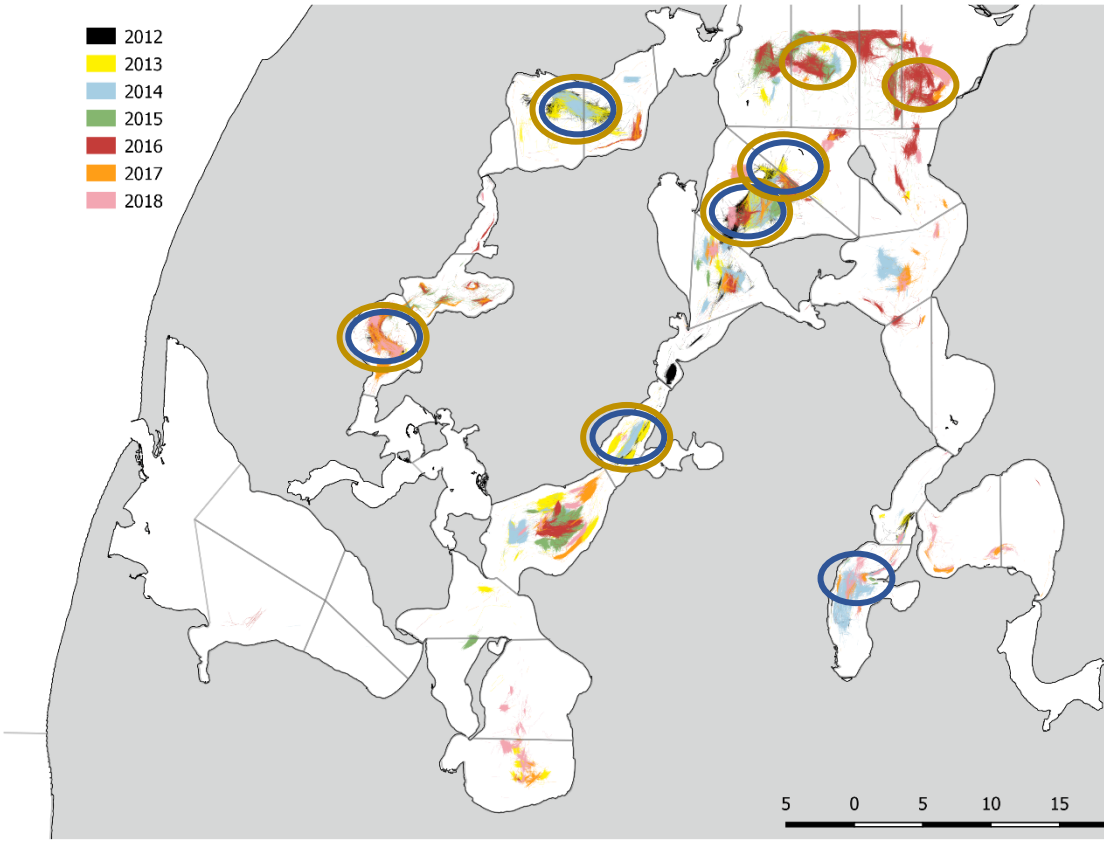

Figure 5.1. Map of the Limfjorden. Grey lines delimitate the fishing areas. Each colour represents the cumulated information on the mussel fishing tracks between 2012 and 2018 from black box data. The blue circles show the areas where fishing takes place after two to three years while the brown circle areas where fishing takes place on consecutive years

Mussel beds act as protecting reefs against predators (crabs, starfish, sand slug; Okamura, 1986) and potential dislocation from currents (Bertness and Grosholz, 1985, Murray et al., 2002; predation). However self-organisation in mussel beds can also be detrimental with intraspecific competition for food (van de Koppel et al., 2005, Okamura, 1986, Saurel et al 2013). The following hypothesis were tested using a dual approach, namely in situ experiments and modelling.

1. There are no larvae in the water column going to the unfished areas:
2. Fishing creates optimal substratum for spat settlement:
3. Fished beds improve mussel recruitment by reducing competition for food and space, and removing predators.

In areas where mussels historically were present in high densities and disappeared once the fishery was closed (Agerø, Dinesen et al. 2015), spat collectors were placed to see whether larvae were still present in the water. In Thisted broad where anoxic conditions occur during the summer period, experimental dredging was conducted to investigate the potential impact of gear on damaged bed by disturbing the anoxic layer and re-oxygenating the surface sediment. In Løgstør Bredning, a large-scale dredging experiment was carried out in an area with mussel beds (Løgstør 17) to survey the potential recolonization of the recently fished tracks by new mussel spat. To support this, BACI experiments (Before-After-Control-Impact) were conducted to assess the impact of dredging on a bed vs non-dredged bed for new recruitment and population distribution. Finally, in order to investigate the potential mussel settlement in mussel beds fished one to two years previously, the population structure was estimated in two sites in Løgstør Bredning (Løgstør 15 and 16). At each site, spat collectors were placed both in the water column and close to the mussel bed in fished vs pristine areas. The second approach used the FlexSem model tool developed during the project (see section 2.2), where a larvae dispersal model was set up to determine mussel larvae transport in the Limfjorden, using existing monitored mussel beds as source of larvae.

5.2 Mussel recruitment in the Limfjorden[5]

5.2.1 Field work

The five experimental sites are presented in Figure 5.2 and Table 5.1. At each site, a single longline was installed with spat collectors of 2 m length and 5 cm wide, together with a structure including both a caged area vs uncaged area at the bottom of the water column. Cage structures were made of iron bars (diameter: 1 cm, dimensions: 80 x 100 x 50 mm). Half of the structure was protected with a cage made with a plastic net (mesh size: 5 mm) pushed inside the sediment (h > 3 cm) to avoid predator entering the netted area. In each cage, two spat collectors: 50 cm x 5 cm were attached in both protected and unprotected structure. On each line were hanged six spat collectors 2 m x 5 cm. Depending on the site, series of spat collectors were deployed in May, June, July and August and removed in June, July, August and September in order to catch different spat settlements.

[5] Part of this study has been submitted in Journal of Sea Research as: Bromhall K., Dinesen G.E., McLaverty, C.; Eigaard, O.R., Petersen, J.K. and C. Saurel. Experimental effects of a lightweight mussel dredge on benthic fauna in a eutrophic Natura 2000 site.

Table 5.1. Site description for the mussel spat recruitment experiment.

Sites	Description	Coordinates	Test hypothesis
Site 1 – Agerø:	Unfished for 30 years, mussels have disappeared from the bottom. One experimental fish track. Only one set of longline.	56° 43.700´N 008° 31.900´Ø	1, 2b, and 3b
Site 2 – Thisted:	Bed marked by anoxic event with dead mussels. One experimental fish track to remove surface layer. Only one set of longline.	56° 55,900´N 008° 44,000´Ø	1, 3c
Site 3– Løgstør 2015 St4: fished St5: unfished	Unfished in Natura 2000 vs fished in 2015. Stations approx. 100m apart. Note unfished area few bivalve.	St4: 56° 58,724´N 009° 05,334´Ø St5: 56° 58,953´N 009° 05,325´Ø	1, 2a, 2b, 3a.
Site 4 - Løgstør 2016 St10: fished St8: unfished	Unfished in Natura 2000 vs fished in 2016. Stations approx. 2000m apart. Note unfished area few bivalves, mainly cockles and some mussels.	St10: 56° 58.384´N 009° 09.863´Ø St 8: 56° 58.987´N 9° 09.8956´Ø	1, 2a, 2b, 3a
Site 5 - Løgstør 2017 Unfished Fished	Unfished area vs fished area in May 2017 for the project by the Limfjorden vessel (1 ha and 185t removed), close to each other.	56° 57.270´N 009° 10.600´Ø	1, 2a, 2b, 3a

Figure 5.2. Limfjorden map with the sampling station for mussel spat recruitment during May to September 2019.

Spat collectors were retrieved by a diver. In mussel beds in Løgstør, quadrats (2500 cm^2) and in Løgstør 17 cores (145 cm^2) were taken by the diver to study the mussel density and shell length distribution at the beginning of the season before recruitment was occurring and at the end of the season.

All samples were transported back to the DSC laboratory for further analysis. Spat collectors were weighed and then species attached were identified, counted, and weighed, quadrat samples were weighed and sorted. In total there could be up to 10 treatments per site as a combination of the following: Fished (F), Unfished (UF), protected in the cage (C), unprotected from the cage (UC), on top of bare sediment patches (B), on top of mussel patches (M), and longlines. Treatments: 1) F_C_B, 2) F_UC_B, 3) F_C_M, 4) F_C_B, 5) UF_C_B, 6) UF_UC_B, 7) UF_C_M, 8) UF_C_B, 9) F_longline, 10) UF_longline. The period of deployment is indicated such as MJ (May to June), MS (May to September), JJul (June to July).

5.2.2 Mussel spat recruitment results

There was mussel recruitment in all experimental sites for each of the deployment periods (May, June and July) on the spat collectors placed in the water column (Figure 5.3). In all sites, after the first month of deployment, mussel density was between 60 and 140 g m^{-1}. In contrary, there was hardly any mussel recruitment on the spat collectors placed at the bottom (Figure 5.4).

Spat were present in both fished and unfished areas and in Agerø, which is a site known for the disappearance of its mussel beds (Dinesen et al. 2015). In Løgstør 2015 there was more spat recruited in the water column in the unfished area, while this trend was the reverse in Løgstør 2016. In Løgstør 17, recruitment occurred in May, June and July, as seen in the Figure 5.3.

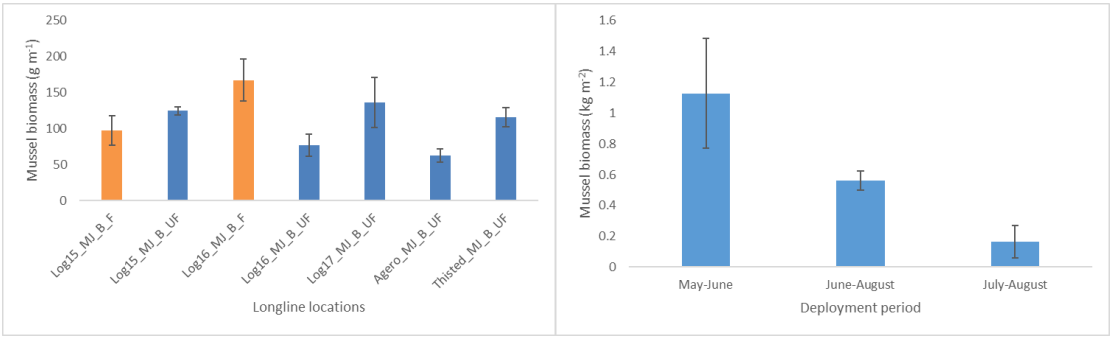

Figure 5.3. A. Mussel biomass in g m^{-1} of spat collectors placed on longlines. Log for Løgstør stations, MJ for May to June deployment. Orange indicate longline in Fished areas, while blue is for unfished areas. In both Løgstør 17, Agerø and Thisted, only one longline was placed and thus considered as fished and unfished treatment. B. Mussel biomass in g m^{-1} of spat collectors placed on longline in Løgstør 17 deployed during three different period in 2017.

The results of the benthic spat collectors are different from the water column. Mussel spats were only found on 13 spat collectors out of the >100 benthic spat collectors deployed (Figure 5.4). No mussel was found on the spat collectors deployed in Løgstør 16 from all treatments. Only one spat collector presented mussels in Løgstør 15 unfished area, out of a total of 24 spat collectors deployed. Two spat collectors out of 11 presented mussels in Thisted, while 5 in 12 in Agerø. In Løgstør 17, 7 out of 29 spat collectors had mussels. For all stations, except for Løgstør 16, there was recruitment on the spat collectors during the May-June period (Figure 5.4).

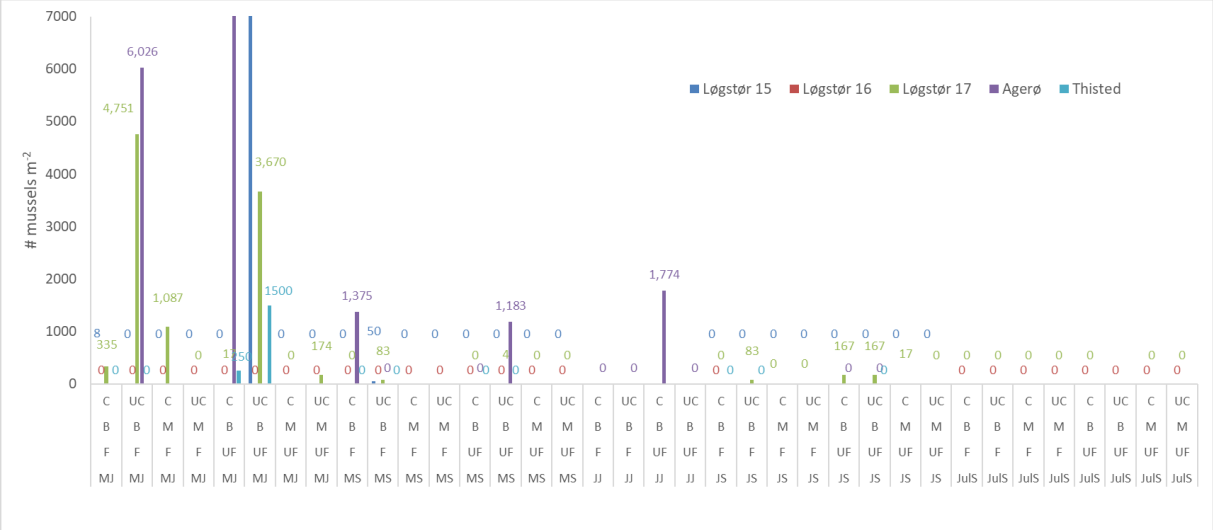

Figure 5.4. Mussel count per m^{-2} at different period of deployment in benthic spat collectors in cage (C) or unprotected (UC), on bare (B) or mussel (M) patches, in fished (F) or unfished (UF) areas for the five different experimental stations. M: May, J: June, Jul: July, S: September.

The proportion of the different species recorded by sites is presented in Figures 5.5 & 5.6, with results at different time of deployment. In Agerø, there was a succession of barnacles, ascidians *C. intestinalis* and mussels in May-June while the community shifted later toward the ascidians *A. aspersa*, *C. intestinalis* and some starfish later between May-September. Another mussel recruitment happened on the spat collectors inside some cages between June and July 2017. Thisted had some mussel recruitment between May-June, but they disappeared by September in favour of ascidians and barnacles with some spat collectors washed up of species.

In Løgstør 15, mussel recruitment only occurred in May and in only one unprotected spat collector (UF-B-UC). No other species were identified on the collectors. Thereafter, annelid worm *P. triqueter* and ascidian *A. aspersa* were dominating the coverage on the spat collectors and this was site specific. *A. aspersa* was mostly present in the fished area and *P. triqueter* in the unfished area. Results in Løgstør 16 are similar to Løgstør 15, with no visible mussel recruitment and a dominance of the ascidian *A. aspersa* in the fished area vs *P. triqueter* in the unfished area. In Løgstør 17, a similar dominance of ascidians and *P. triqueter* with no mussel spats was recorded in September.

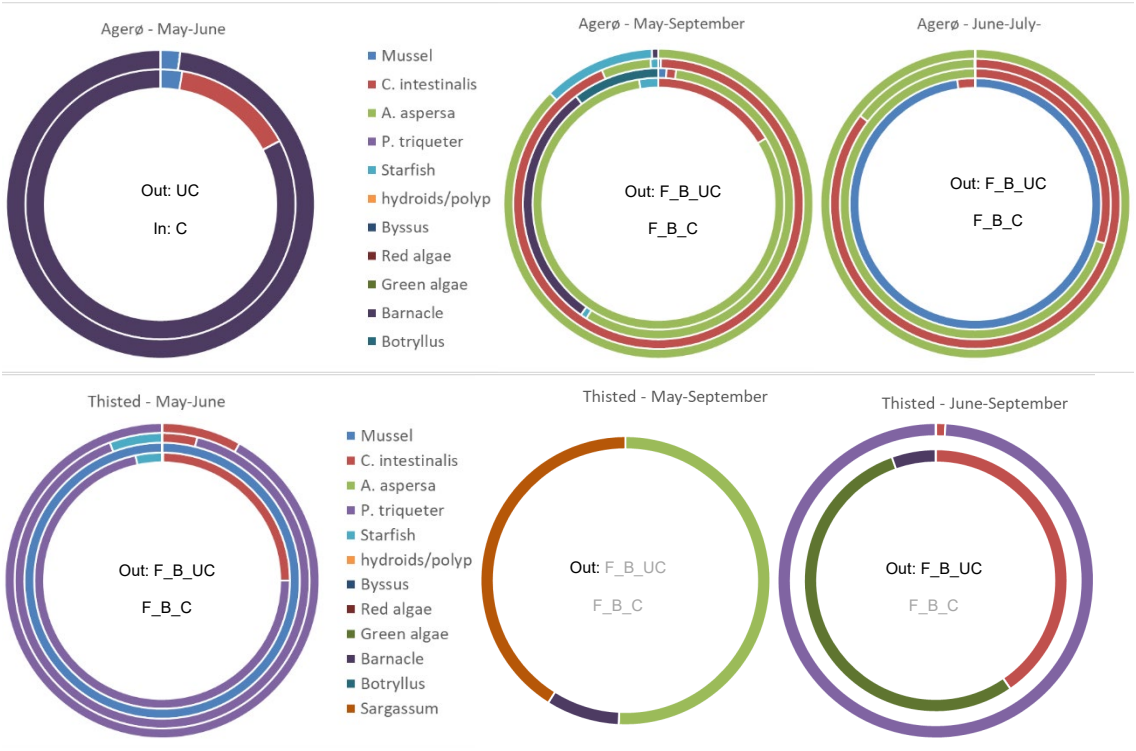

Figure 5.5. Relative weight of different organisms identified on the spat collectors in Thisted and Agerø. Spat collectors in cage (C) or unprotected (UC), on bare (B) or mussel (M) patches, in fished (F) or un-fished (UF) areas. In grey, no species recorded on the spat collector.

While the spat collectors placed at the bottom did not have a high recruitment of mussels, potentially due to cage effect and predation, the result of the recruitment in the mussel bed from samples taken with quadrats (Løgstør 15, 16 and 17) and cores (Løgstør 17) indicated some recruitment to the bed. Only Løgstør 16 and 17 had some small spat (< 20mm) in September 2019 (Figure 5.7). A more detailed analyse of the shell length at different time and treatment is presented in both Table 5.2 and Figure 5.8.

Figure 5.6. Relative weight of different organisms identified on the spat collectors in Løgstør 15, Løgstør 16, Løgstør 17, Spat collectors in cage (C) or unprotected (UC), on bare (B) or mussel (M) patches, in fished (F) or unfished (UF) areas. In grey, no species recorded on the spat collector.

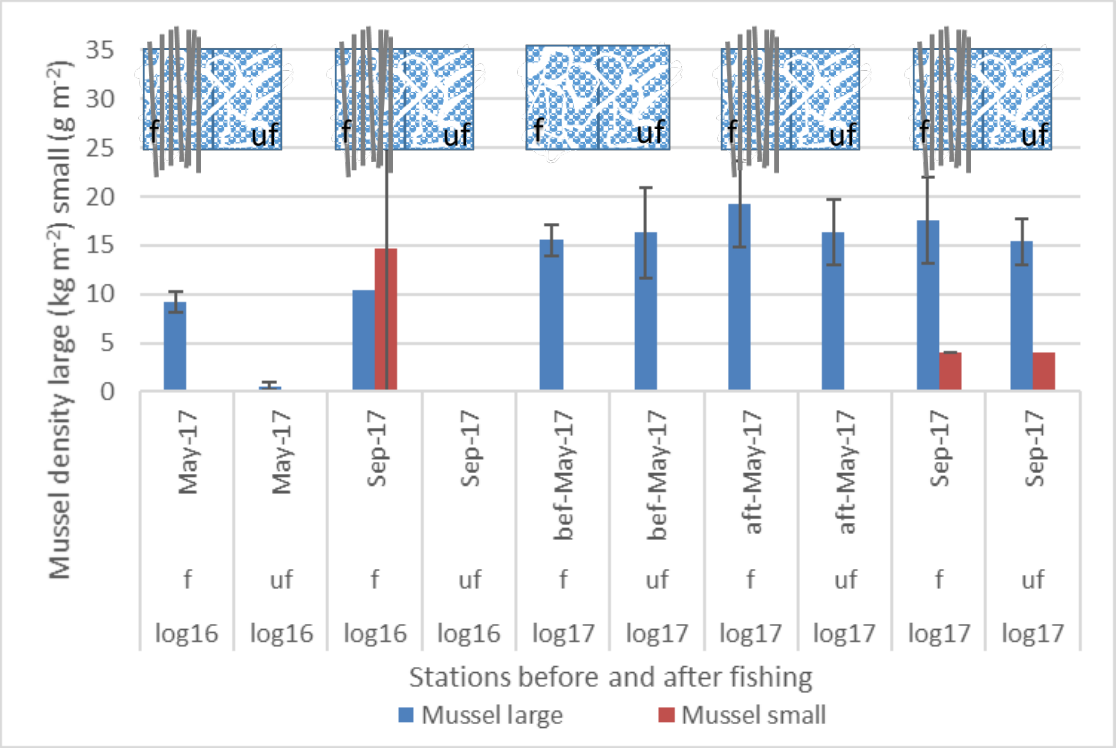

Figure 5.7. Mussel bed density in the sampling station of Løgstør 16 and Løgstør 17, bef: mid-May 2017 before fishing in Løgstør 17, aft and aft2 correspond to sampling in September 2017, aft1 is at the end of May. f = fished area, uf = unfished area. Large mussels, weight in kg, small mussel, weight in g.

In Figure 5.8 results for Løgstør 16 and 17 as boxplot of mussel shell length (mm) indicate that the standard deviation of the Q1 (lower part of the box) is larger than for Q3 (upper part of the box) with a larger deviation after fishery, indicating that there are more small mussels in the population.

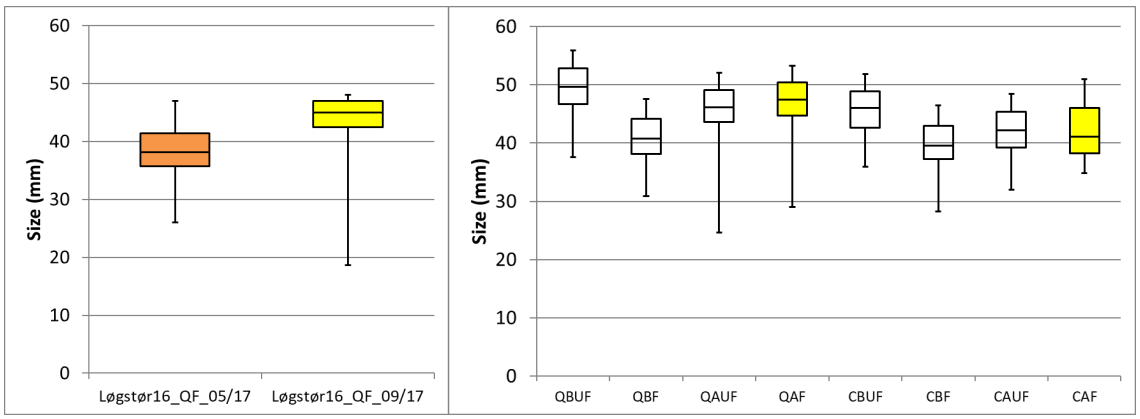

Figure 5.8. Boxplot of mussel shell length (mm) in a) Løgstør 16 in May and September 2017 both the year after fishing and b) Løgstør 17 sampled from quadrats in May (before fishing occured) and September (After fishing occured) 2017. Q: quadrat, C: core, B: before, A: after, F: fished, UF: unfished.

In Løgstør 17, the comparison between quadrats and core methods taken simultaneously showed that for the same treatment, the mean shell length from the quadrats was statistically ($p < 0.01$) superior to the mean shell length of the cores. This could be explained by the smaller surface sampled by

the cores (145 cm^2) in comparison to the quadrats (2500 cm^2). However, the various trends and differences between sampling time or treatment (fished vs unfished) were statistically not different (Table 5.2).

Table 5.2. Quadrats and cores results in Løgstør 17 before and after fishing. Descriptive statistics and 2 sample t-test between the various treatments. Letter in order of apparition: C = Core, Q = Quadrat, A = after, B = Before, UF = unfished, F = fished

Variable	N	Mean SL	StDev SL	Mean Ind. m^{-2}	Mean weight m^{-2}
CAUF	177	42.388	4.875		
CAF	248	42.948	4.689		
CBUF	200	45.629	4.86		
CBF	251	39.904	4.867		
QAUF	1344	46.215	4.578	2047	15.37
QAF	1406	47.345	4.479	2173	17.56
QBUF	300	49.712	4.574	1964	16.33
QBF	300	40.981	4.756	3324	15.52

2-samples T-test results for shell length comparison:			
Core	Fish/unfished	CBF < CBUF	CAF = CAUF
		T_{437} = -12.5, p < 0.001	T_{367} = 1.21, p = 0.226
Quadrat	Fish/unfished	QBF < QBUF	QAF > QAUF
		T_{587} = -22.8, p < 0.001	T_{2728} = 6.49, p < 0.001
Core	Before/after	CAUF < CBUF	CAF > CBF
		T_{365} = -6.4, p < 0.001	T_{495} = 7.17, p < 0.001
Quadrat	Before/after	QAUF < QBUF	QAF > QBF
		T_{458} = -12.1, p < 0.001	T_{405} = 20.7, p < 0.001

Before the fishing took place, mussels were statistically on average 9 mm bigger (for quadrat sampling) in the control site than in the future fished site (Table 5.2). However, few months after fishing, the mussels grew more in the fished site. Mussel density presented in Figure 5.9 indicates that there were more individuals m^{-2} in the fished area before the fishing took place in May than in the control site unfished, however, there were no statistical difference between all the treatments (ANOVA analysis of site, time, interaction site and time, $p > 0.05$). Individuals were statistically smaller and lighter at both recovery and after a few months (Table 5.2 & Figure 5.9). After fishing, the mussel density as number of individuals m^{-2} reduced as it would be expected from the fishery. Mussels seemed to grow bigger than in the control unfished site (Table 5.2 & Figure 5.9) as supported by statistical results for shell length.

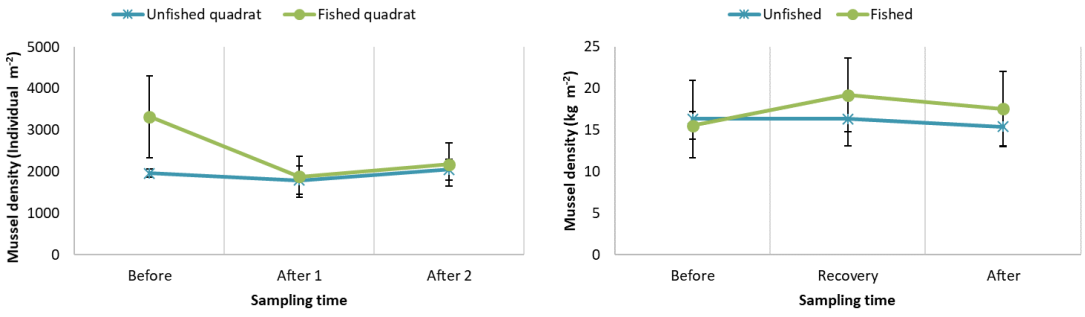

Figure 5.9. Mussel density recorded as count m^{-2} or kg m^{-2} in Løgstør 17 sampled from quadrats in May (Before), just after fishery in May (Recovery) and September (After) 2017.

Overall, fishing seems to improve mussel bed growth, but there is no direct evidence in this study of improved mussel recruitment on fished beds as seen in the Figure 5.10 with a small amount of new small mussels visible in the shell length frequency diagram.

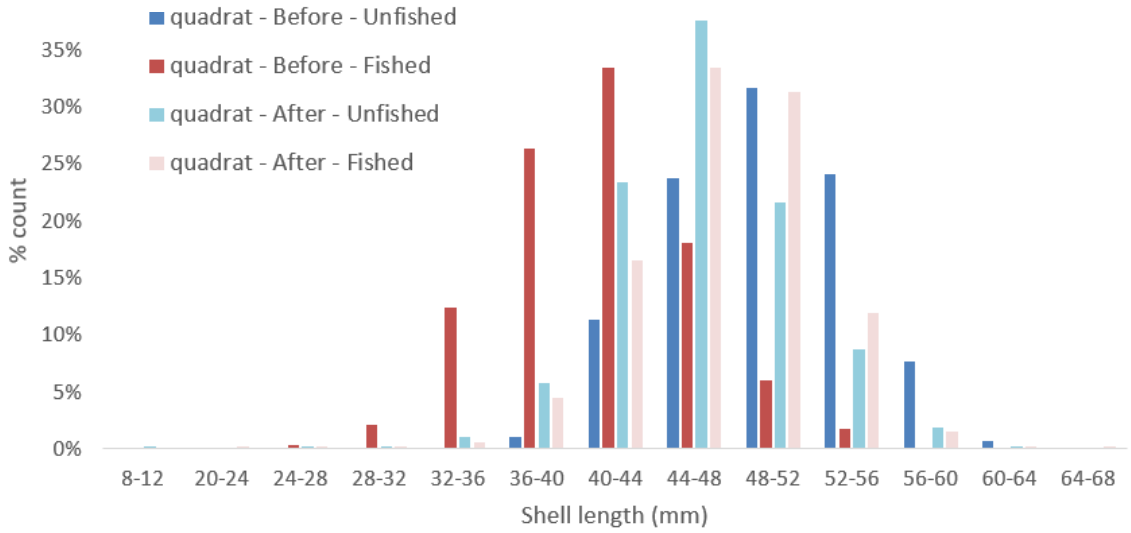

Figure 5.10. Shell length frequency Løgstør 17 sampled from quadrats in May (Before fishing) and September (After fishing) 2017 in the fished and unfished areas.

5.3 Larvae dispersal model and results[6]

The aim of the model study was to determine mussel larvae transport (after spawning) from the mussel beds to the final locations for settling. Connectivity is defined as the exchange of individuals among geographically separated populations. Hence, the estimated connectivity can be used to identify areas that are the main donors and receivers of larvae and if some areas are physically isolated. In order to examine the connectivity between sub-areas in the Limfjorden, an Agent Based Model (ABM) was coupled to the 3D hydrodynamic model FlexSem Limfjorden setup. The Limfjorden model has two open boundaries exchanging water with the North Sea to the west and Kattegat to the east. Initial fields and open boundary forcing of water level, horizontal velocities, temperature and salinity were obtained from the HBM model (see section 2.1). In the ABM approach, individual agents are transported around in the 3D model domain. Each agent can have its own model and interact with the 3D model environment. In each ABM timestep, the 3D Eulerian velocities are interpolated to the positions of the agents, which then are advected in a Lagrangian way. The velocities from the unstructured mesh are interpolated using an area-weighted approach (Wang et al. 2011).

Mussel larvae were defined by two biological parameters: i) the pelagic larval duration (PLD), which was set to 11, 18, 21, 32, 39 and 46 days, to test the model response to different length periods for the larvae in the water column and ii) a main spawning event in May. To simulate the dispersion of mussel larvae, we used numerical particles released from the mussel bed sampling stations acting like a source area (Figure 5.11). The particles were released in the surface and then moved freely in the water column after each release. A total of 33,000 particles were released during the main spawning event in May subdivided into four releases, one every week of 8250 particles each. Each particle represents a super-individual consisting of multiple larvae. The mussel densities at the stations were considered for the number of larvae released. The individual trajectories of the particles were stored for the extent of the pelagic phase. No random vertical or horizontal movements of the particles were included in the simulations. At the end of the PLD, settling occurred once for particles ending anywhere within the model domain. The Limfjorden was divided into 17 sub-areas based on the administrative fishing areas, where some areas were merged due to similarities in the physics and occurrence

[6] Part of this study has been published in: Pastor et al. 2021 Agent-based modeling and genetics reveal the Limfjorden as a well-connected system for mussel larvae. MEPS. DOI: 10.3354/meps13559

of mussel beds. The total number of simulated larvae successfully settling in each sub-area was calculated and assumed to represent the potential recruitment. No mortality due to e.g. predation was considered and the actual recruitment is likely lower than the model estimates.

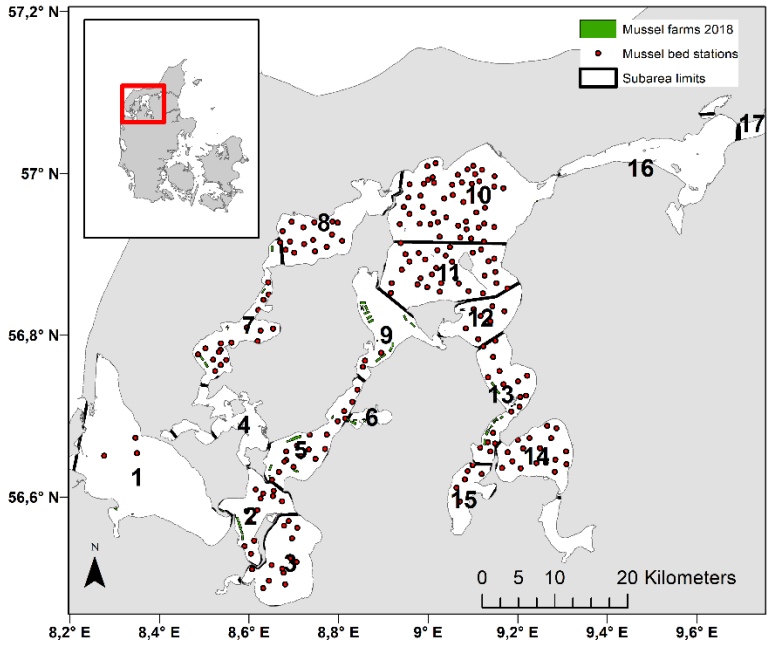

Figure 5.11. Map of the sampling stations (red dots) of mussel beds in the Limfjorden. The Limfjorden is divided into 17 sub-areas for the connectivity study (sub-area limits shown in black).

The results were summarized as a connectivity matrix for the pelagic larval duration of 21 days, which is assumed to be the most realistic duration according to field studies (Figure 5.12). Preliminary results on larval connectivity in the area showed that there was a high probability of the larvae to settle in the same sub-area, where they were originally released. This is defined as self-recruitment (shown as diagonal values in the connectivity matrix). This was the case in all sub-areas, except where no mussels were released (area no. 1, 2, 4, 6, 16 and 17). Self-recruitment was higher for short PLDs, and as we increase the number of days that the larvae remain in the water column, larvae will move longer distances to other areas within the Limfjorden (results not shown). Main donor and receiver areas were identified by the model for the different scenarios. For year 2010, area 5 corresponding to Kås Bredning was the main donor area and areas 10 and 11 (Løgstør Bredning) and 13 (Risgårde Bredning) appeared to be the main receiver areas. These connectivity results can be explained by the physical circulation patterns in the area (Figure 5.13). The modelled mean current speed and standard deviation during the study month was highest in the narrow strait of Kås Bredning (area 5), which caused a higher export of larvae. Løgstør Bredning was a larger area with many mussel beds and low current speeds contributing to the high self-recruitment. Area 6, Lysen Bredning, seemed to be rather isolated only receiving a few larvae from the neighbour Kås Bredning.

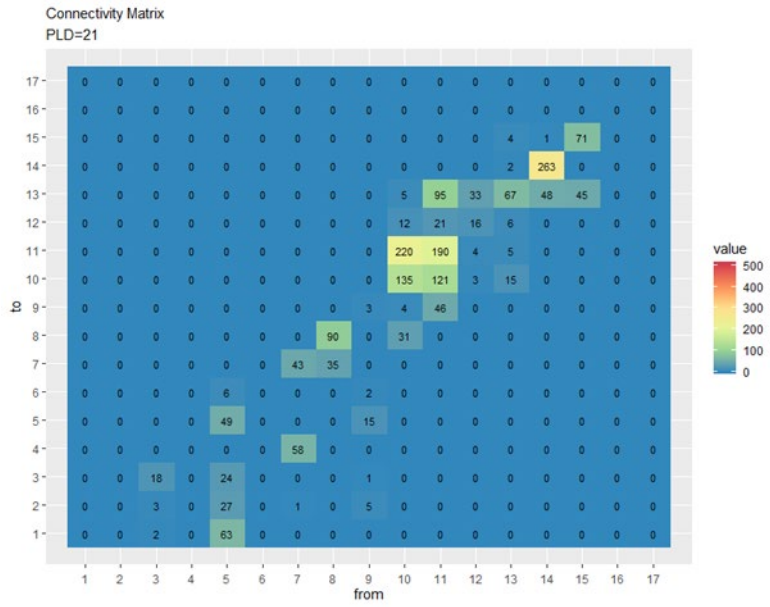

Figure 5.12. Connectivity matrices for the 17 water bodies in 2010. The colour code indicates the probability to be connected to a specific water body with the diagonal elements being the probability of the larvae to stay in the same area (self-recruitment). PLD: Pelagic Larval Duration (Modified from Pastor et al. 2021).

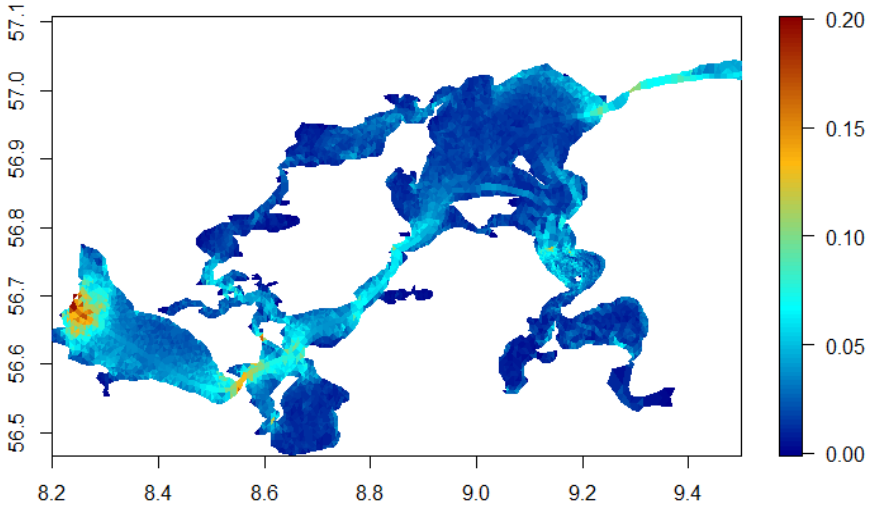

Figure 5.13. FlexSem physical model showing the mean current speeds (m s^{-1}) in the Limfjorden year 2010 (Modified from Pastor et al. 2021).

5.4 Discussion

The experimental approach established that there were many mussel larvae in the water column settling on suspended spat collectors in the five chosen sites, and it validated some results of the model simulating the larvae dispersal and connectivity regarding the location of larvae ready to settle as

seen in Figure 5.14. Experimental stations for mussel recruitment are superimposed with one or more output from the larval dispersion model.

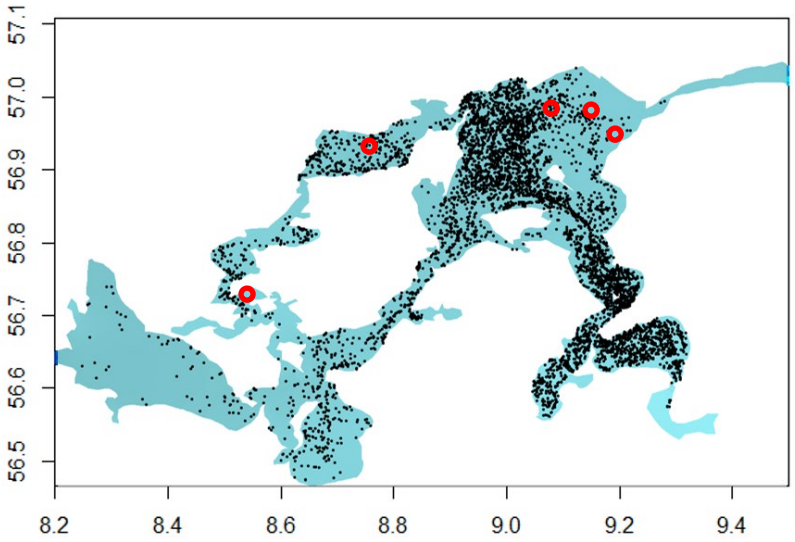

Figure 5.14. Map of the sampling stations (red empty circles) of experimental station with spat collectors in the water column mussel in the Limfjorden together with positions of mussel larvae ready to settle (black dots) estimated by the larval dispersal model.

The large presence of larvae in the water column measured via successful settlement of larvae on suspended spat collectors as a proxy is an asset to the Limfjorden and beneficial to the longline aquaculture. This success can be attributed to i) almost no predation in the water column, 2) use of appropriate material for spat settlement, and 3) deployment at the right period of the year for spat recruitment. The success of mussel settlement at all stations is also very encouraging as it indicates that there might not be a shortage of mussel larvae in the Limfjorden, but rather an issue for settlement on the bottom, which is likely due to a combination of several factors.

Mussel settlement at the bottom of the Limfjorden proved to be more problematic and although in the past 10 years it has been decreasing (fishermen pers. comm.) resulting in a decrease of the population (Nielsen et al. 2018), recruitment seems to be going up again in 2020-2021 (fishermen pers. comm.). The scarcity of mussel spats present on spat collectors positioned at the bottom of the water column could be explained by several factors: 1) the presence of predators at the bottom for unprotected spat collectors, 2) cage effect with reduced flux of food and oxygen due to biofouling with a negative effect on spat survival in the cage, 3) permeability for predator larvae such as starfish to enter the cages, 3) intraspecific competition for food with larger mussels from the bed, and 4) other species settlement succession and competition for space on the spat collectors. Moreover, diving was conducted to clean the nets from biofouling of the net of the cages during July to avoid nets clogging by especially ascidians. During sampling, large amounts of crabs, starfish and sea slugs were also spotted close by and on top of the cages and on the unprotected spat collectors. The spat collector methodology offers little refugee to the spat in comparison with the matrix created by the mussel bed (Murray et al., 2002). There is also a general trend observed by fishermen of an increase of the crab population in the Limfjorden, and the starfish population is also thriving with large front devastating cockle and mussel beds. In Agerø, no mussels were found at the bottom, however many predators and ascidians were present. In Thisted Bredning, the experimental stations were selected with the

help of the fishermen. They had black anoxic sediments with little visibility close to the bed, suggesting that the fishing track might not have been sufficient to improve the surface area properties for mussel recruitment and presenting potentially adverse conditions for mussel survival.

The biofouling species seemed more opportunistic in the presence of predators to colonise more efficiently the bottom spat collectors in comparison with the suspended ones. It is interesting to notice that depending on the site and the time of deployment and level of protection from predators/current flow, different communities of species settled on the larvae. The dominant species were *P. triqueter*, and both ascidians species *C. intestinalis* and *A. aspersa*

The population structure from quadrat and core surveys showed the same trends in mussel density, population structure, which suggest that the methodology was more adapted to studying mussel recruitment in mussel beds only. Shell length increased statistically significantly in the fished area (Løgstør 2017). Although the number of individual mussels per m^{-2} seemed to decrease after fishing, while weight per m^{-2} seemed to increase, there was no statistically significant difference. This could be an indication that there was less competition for food and mussel grew bigger and faster. In the control area, the opposite trend was observed: the number of individual mussels per m^{-2} increased at the end of the experiment, while the weight per m^{-2} decreased, but again with no statistically significant difference. It is difficult to see from the samples if some of the removal from the fishery has been replaced by new recruitment.

These results pave the road for a more extensive survey of both mussel beds before and after fishing with higher sampling intensity to account for the high variability of density in mussel beds in order to study the thinning effect on mussel bed productivity. More emphasis on the impact of predators to the mussel recruitment in mussel beds and bare beds amongst others should be given to determine the factors responsible for the low amount of mussel recruitment at the bottom.

6. Recommendation to management

Mussel fishery in Danish waters in general and in Limfjorden especially is managed by a number of different regulatory mechanisms with a general overarching reference to the mussel policy. Hitherto the mussel policy has had a focus on the direct physical impact of the mussel dredge on key ecosystem components like eelgrass, macroalgae, benthic fauna and structuring elements like stone reefs. However, it has been recognized that the fishery also has some indirect effects in the ecosystem of which some can be considered potentially damaging, like resuspension of sediments during dredging causing enhanced light extinction in the water column and thus adverse light conditions, e.g. eelgrass. But there could also potentially be beneficial effects related to, e.g. transplantation of mussels from areas often exposed to oxygen depletion.

With the present study, new knowledge has been achieved regarding sediment dispersal in relation to mussel dredging, potential effects of mussel relay practice where mussels are transplanted from areas with poor growth conditions to areas with more favourable conditions and potential effects of dredging on mussel recruitment. The results of the project lead to some recommendations related to indirect effects of mussel fishery:

- Only a few eelgrass boxes in the study areas are close to mussel beds of interest to the fishermen, while for most of the boxes, the fishery is occurring further than 500 meters from their borders. Under new management scenarios, the current standard 300 meter buffer zone around eelgrass beds established to protect for effects of resuspension could be reduced, but not less than 100 m to prevent potential direct effects, such as is the case for geogenic reefs in Natura 2000 areas (Pers. Comm. Danish Fishery Agency). They could be replaced by site-specific buffer zones reflecting sediment characteristics and hydrodynamic conditions in the area where buffer zones are part of the management plans. Further, given the relatively short plume duration even for smaller particle fractions, the indirect effects of mussel dredging relating to impoverished light regimes can be considered small and mainly related to intensity and duration of the fishery and of the fishing season, i.e. if the fishery takes place in the growing season for eelgrass. Buffer zones around eelgrass beds could thus be established primarily to prevent the direct physical impact of the fishing gear and/or to allow for a slow increase in maximal depth or extension of the eelgrass beds. This will require site-specific buffer zones, at least in Natura 2000 areas.

- Using Lovns Bredning as a case study, it can be concluded from a modelling exercise that transplanting mussels from areas often exposed to oxygen depletion will have some added environmental effects besides the direct impact of the dredging on the bottom. The main effects are an immediate increase in bottom oxygen concentration from the reduction of mussel biomass and the associated oxygen consumption from bacterial degradation of mussel killed by anoxia, and subsequent decrease in nutrient and Chl. *a* concentrations leading to increase Secchi depth. Mussel biomass was reduced as a direct effect of the transplantation but soon recovered. Given these results, it is recommended that permits to transplant mussels from areas like Lovns Bredning are managed carefully in view of the potentially positive effects related to the transplant and not only the adverse effects related to the dredging activity such as loss of biodiversity and release of CO_2 *sensu* Sala et al 2021. Further, environmental management should consider if the removal of mussels from areas like Lovns Bredning can be part of an environmental management plan for improving general ecological status.

- In the present project, we could not document a direct link between fishery and mussel recruitment. This was most likely due to an overriding phenomenon observed in both Limfjorden and other mussel fishing districts along the Jutland east coast of generally reduced recruitment to blue mussel beds. This tendency is most likely caused by increased predation pressure (e.g. starfish, shore crab), as also observed in the present study. It can thus be recommended that further investigations on the predation pressure on natural mussel beds are initiated to secure future fisheries. Even though recruitment was not directly linked to fishery, it should be noted that the current fishery results in thinning of dense beds thereby optimizing cumulated yield of the beds and reducing cumulated bottom impact.

7. Dissemination

Murawski J, She J, Mohn C, Frishfelds V and Nielsen JW (2021) Ocean Circulation Model Applications for the Estuary-Coastal-Open Sea Continuum.Front. Mar. Sci. 8:657720.
doi: 10.3389/fmars.2021.657720

Maar, M., Larsen, J., Saurel, C., Mohn, C., Murawski, J., & Petersen, J. K. (2021). Mussel transplantation as a tool to mitigate hypoxia in eutrophic areas. *Hydrobiologia*, *848*, 1553-1573. https://doi.org/10.1007/s10750-021-04545-6

Maar, M., Larsen, J., Saurel, C., Mohn, C., Murawski, J., & Petersen, J. K. (2021). Mussel transplantation as a tool to mitigate hypoxia in eutrophic areas. ASLO June 2021, virtual meeting.

Pastor Rollan, A., Maar, M., Larsen, J., Saurel, C., & Petersen, J. K. (2020). *Modelling mussel larval distribution in the Limfjord for optimal site selections of mussel farming*. Abstract from ocean sciences meeting 2020, San Diego, United States. https://agu.confex.com/agu/osm20/meetingapp.cgi/Paper/642895

Pastor, A., Larsen, J., Mohn, C., Saurel, C., Petersen, J. K., & Maar, M. (2020). Sediment Transport Model Quantifies Plume Length and Light Conditions From Mussel Dredging. *Frontiers in Marine Science*, *7*, [576530]. https://doi.org/10.3389/fmars.2020.576530

Pastor Rollan, A., Maar, M., Larsen, J., Saurel, C., & Petersen, J. K. (2019). Modelling mussel larval distribution for optimal site selections of mussel farming. In *20. Danske Havforskermøde Abstractkatalog* (pp. 208-208). Syddansk Universitetsforlag. https://www.dhm2019.dk/

Pastor Rollan, A., Maar, M., Larsen, J., Saurel, C., & Petersen, J. K. (2019). Modelling mussel larval distribution for optimal site selections of mussel farming. In *Aquaculture Europe 2019: Our Future Growing From Water* (pp. 1122-1123). European Aquaculture Society. Aquaculture Europe 2019, Berlin

Saurel, Camille; Mohn, Christian; Andersen, Kasper; Andersen, Lars; Bak, Finn; Barreau, Pascal; Larsen, Janus; Maar, Marie; Nielsen, Niels Peter; Pastor, Ane; Petersen, Jens Kjerulf (2021): Water currents and light intensity data for estimating sediment plume size and light conditions from mussel dredging in two areas of the Limfjorden, Denmark. PANGAEA, https://doi.org/10.1594/PANGAEA.927135

Saurel, C., Mohn, C., Andersen, K. L., Pastor Rollan, A., Maar, M., Larsen, J., Bak, F., Barreau, P. D. A., & Petersen, J. K. (2019). *Sediment transport and dispersal during mussel fishery*. Abstract from Dansk Havforskermøde 2019, Odense, Denmark.

Saurel, C., Mohn, C., Andersen, K. L., Bak, F., Barreau, P. D. A., & Petersen, J. K. (2017). *Estimation of potential indirect effects of sediment transport from mussel seed fisheries on eelgrass beds*. Abstract from Aquaculture Europe 2017, Dubrovnik, Croatia.

References

André C, PR Jonsson and M Lindegarth (1993) Predation on settling bivalve larvae by benthic suspension feeders: the role of hydrodynamics and larval behaviour. Marine Ecology Progress Series 97:183–192.

Asmus RM and H Asmus (1991) Mussel beds -limiting or promoting phytoplankton. J Exp Mar Biol Ecol 148:215-232.

Berg P (2012). “Mixing in HBM. DMI Scientific Report No. 12-03”. Copenhagen, 21 pp. (Available at: www.dmi.dk/file8admin/Rapporter/ SR/sr12-03.pdf).

Berg P, and J Weismann Poulsen (2012). Implementation details for HBM. DMI Technical Report No. 12-11. Copenhagen, 149 pp. (Available at: www.dmi.dk/fileadmin/ Rapporter/TR/tr12-11.pdf).

Bertness, M and E Grosholz (1985) Population dynamics of the ribbed mussel,Geukensia demissa: The costs and benefits of an aggregated distribution.Oecologia. 67:192-204.

Boström C, S Baden, A-C Bockelmann, K Dromph, S Fredriksen, C Gustafsson, et al. (2014) Distribution, structure and function of Nordic eelgrass (*Zostera marina*) ecosystems: implications for coastal management and conservation. Aquat. Conserv. Mar. Freshwat. Ecosyst. 24, 410–434. doi: 10.1002/aqc.2424.

Carstensen J, D Krause-Jensen, S Markager, K Timmermann and J Windolf (2013) Water clarity and eelgrass responses to nitrogen reductions in the eutrophic Skive Fjord, Denmark. Hydrobiologia 704:293-309.

Christoffersen M, P Dolmer, HT Christensen, K Geitner and N Holm (2012) Konsekvensvurdering af fiskeri på blåmuslinger i Lovns Bredning 2012/2013. DTU Aqua-rapport nr. 257-2012. Institut for Akvatiske Ressourcer, Danmarks Tekniske Universitet:77.

Danish AgriFish Agency 2016. Fisheries inspection 2015, Commercial and recreational, Inspection and results. Report 24pp.

Dinesen, GE, P Canal-Vergés, P Nielsen, K Filrup, K Geitner, and JK Petersen (2015) Effekter af blåmuslingefiskeri på bundfauna. Institut for Akvatiske Ressourcer, Danmarks Tekniske Universitet. DTU Aqua-rapport, No. 305-2015.

Dolmer P and RP Frandsen (2002) Evaluation of the Danish mussel fishery: suggestions for an ecosystem management approach. Helgol Mar Res 56:13-20.

Dyekjær SM, JK Jensen and E Hoffmann (1995) Mussel dredging and effects on the marine environment. ICES CM /E:13:1-19.

Eigaard OR, RP Frandsen, B Andersen, KM Jensen, LK Poulsen, DB Tørring, F Bak and P Dolmer (2011) Udvikling af skånsomt redskab til fiskeri af blåmuslinger. DTU Aqua-rapport nr 238-2011:1-33.

Eriander L (2017) Light requirements for successful restoration of eelgrass (*Zostera marina* L.) in a high latitude environment – Acclimatization, growth and carbohydrate storage. J. Exp. Mar. Biol. Ecol. 496, 37–48. doi: 10.1016/j. jembe.2017.07.010.

Holmer M, N Ahrensberg and NP Jørgensen (2003) Impacts of mussel dredging on sediment phosphorus dynamics in a eutrophic Danish fjord. Chem Ecol 19:343-361.

Larsen J og JW Nielsen, Denmarks Meteorological Institute technical rapport 01-07, ”Opsætning og kalibrering af Mike21 til stormflodsvarsling for Limfjorden”, 2001, https://www.dmi.dk/fileadmin/user_upload/Rapporter/TR/2001/tr01-07.pdf.

Kamermans P and AC Smaal (2002) Mussel culture and cockle fisheries in The Netherlands: finfing a balance between economy and ecology. J Shellfish Res 21:509-517.

Larsen J, M Maar, T Brüning, J She and C Mohn (2017) Flexsem: a new method for offline ocean modelling. Technical report from DCE-Danish Centre for Environment and Energy, no 105, Roskilde, 1-28:1-28.

Larsen J, C Mohn, AR Pastor and M Maar (2020). A versatile marine modelling tool applied to arctic, temperate and tropical waters. PLoS One 15(4): e0231193.

Lomstein BA, LB Guldberg and J Hansen (2006) Decomposition of Mytilus edulis: The effect on sediment nitrogen and carbon cycling. J Exp Mar Biol Ecol 329:251-264.

Molina-Navarro E, HE Andersen, A Nielsen, H Thodsen and D Trolle (2017) The impact of the objective function in multi-site and multi-variable calibration of the SWAT model. Environ Model Software 93:255-267.

Møhlenberg F (1995) Regulating mechanisms of phytoplankton growth and biomass in a shallow eustary. Ophelia 42:239-256.

Maar M, J Larsen ,K Dahl and B Riemann (2018) Modelling the environmental impacts of future offshore fish farms in the inner Danish waters. Aquaculture Environment Interactions 10:115-133.

Maar M, K Timmermann, JK Petersen, KE Gustafsson and LM Storm (2010) A model study of the regulation of blue mussels by nutrient loadings and water column stability in a shallow estuary, the Limfjorden. J Sea Res 64:322-333.

Murray JMH, A Meadows and PA Meadows (2002) Biogeomorphological implications of microscale interactions between sediment geotechnics and marine benthos: a review. 47:15-30.

Nielsen P, PJ Cranford, M Maar and JK Petersen (2016) Magnitude, spatial scale and optimization of ecosystem services from a nutrient extraction mussel farm in the eutrophic Skive Fjord, Denmark. Aquaculture Environment Interactions 8:311-329.

Nielsen P, K Geitner, J Olsen and MM Nielsen (2018) Notat vedrørende fiskeri af blåmuslinger, søstjerner, europæisk østers og stillehavsøsters i Løgstør Bredning 2018/2019. DTU Aqua report 24 pp.

Nielsen P, MM Nielsen, C McLaverty, K Kristensen, K Geitner, J Olsen, C Saurel and JK Petersen (2021) Management of bivalve fisheries in marine protected areas. Marine Policy, 124: 104357, ISSN: 0308-597X.

Nielsen TG and M Maar (2007) Effects of a blue mussel *Mytilus edulis* bed on vertical distribution and composition of the pelagic food web. Mar Ecol Prog Ser 339:185-198.

Okamura, B (1986). Group living and the effects of spatial position in aggregations of Mytilus edulis. Oecologia. 69:341-347.

Olesen B (1996) Regulation of light attenuation and eelgrass Zostera marina depth distribution in a Danish embayment. Mar. Ecol. Prog. Ser. 134:187–194. doi: 10.3354/meps134187.

Petersen JK, M Maar, T Ysebaert and PMJ Herman (2013) Near-bed gradients in particles and nutrients above a mussel bed in the Limfjorden: influence of physical mixing and mussel filtration. Mar Ecol Prog Ser 490:137-146.

Petersen ME, M Maar, J Larsen, EF Møller and PJ Hansen (2017) Trophic cascades of bottom-up and top-down forcing on nutrients and plankton in the Kattegat, evaluated by modelling. J Mar Syst 169:25-39.

Porri F, T Jordaan, and C D McQuaid (2008) Does cannibalism of larvae by adults affect settlement and connectivity of mussel populations? Estuarine, Coastal and Shelf Science 79:687-693.

Riemann B and E Hoffmann (1991) Ecological consequences of dredging and bottom trawling in the Limfjord, Denmark. Mar Ecol Prog Ser 69:171-178.

Sala, E, J Mayorga, D Bradley, R B Cabral, T B Atwood, A Auber, W Cheung, C Costello, F Ferretti, AM Friedlander, SD Gaines, C Garilao, W Goodell, BS Halpern, A Hinson, K Kaschner, K Kesner-Reyes, F Leprieur, J Mcgowan, LE Morgan, D Mouillot, J Palacios-Abrantes, HP Possingham, KD Rechberger, B Worm, and J Lubchenco (2021) Protecting the global ocean for biodiversity, food and climate. *Nature,* 592:397-402.

Saraiva S, J van der Meer, SALM Kooijman and T Sousa (2011) DEB parameters estimation for *Mytilus edulis*. J Sea Res 66:289-296.

Saurel C, JK Petersen, PJ Wiles and MJ Kaiser. (2013). Turbulent mixing limits mussel feeding: direct estimates of feeding rate and vertical diffusivity. Marine Ecology Progress Series 485:105-121.

She J and J Murawski (2018), “Towards seamless ocean modelling for the Baltic Sea”, Proceedings of the 8-th EuroGOOS international conference: Operational Oceanography serving sustainable marine development, Bergen, Norway, 3-rd to 5-th October 2017.

Tett P (1998) Parameterising a microplankton model, Edinburgh:1-53, IBSN 0902703 609.

Thodsen H, E Molina-Navarro, J Nielsen, J Larsen and M Maar (2018) Afstrømning og næringsstoftilførsler til Limfjorden baseret på tre forskellige modeller. Aarhus Universitet, DCE – Nationalt Center for Miljø og Energi, 20 s. - Teknisk rapport fra DCE -Nationalt Center for Miljø og Energi nr. 115:1-20.

Timmermann K, S Markager and KE Gustafsson (2010) Streams or open sea? Tracing sources and effects of nutrient loadings in a shallow estuary with a 3D hydrodynamic-ecological model. J Mar Syst 82:111-121.

Timmermann K, M Maar, K Bolding, J Windolf, JK Petersen (2019) Mussel production as a tool for nutrient mitigation: Environmental effects on basin scale. Aquaculture Environment Interactions in press 11:191-204.

van de Koppel J, M Rietkerk, N Dankers and PMJ Herman (2005) Scale dependent feedback and regular spatial patterns in young mussel beds. Am. Nat. 165:E66-E77.

Wang B, G Zhao and OB Fringer (2011) Reconstruction of vector fields for semi-Lagrangian advection on unstructured, staggered grids. Ocean Model Online 40:52-71.

Acknowledgements

Foreningen MuslingeErhvervet – FME & Centralforeningen for Limfiorden CF:
Thanks to Viggo Kjølhede, Bo Husted Kjeldgaard, Anders Pedersen and Tommy Gertsen for their help in organising and conducting the fishing experiments, expert knowledge and advices.

DTU Aqua – Dansk Skaldyrcenter:
Thanks to our colleagues for the support and help both in the field, laboratory and discussion. Lars Kyed Andersen, Niels-Peter Nielsen, Martin Veicherts, Mette Møller Nielsen, Paula Canal-Vergés, Pernille Nielsen, Lene Friis Møller, Anita Hansen, Pedro Freitas, Lars Bach Jensen.

The partners:
Danish Meteorological Institute (DMI) and Aarhus University (AU).

The quality assurance reviewers:
Anja Skjoldborg Hansen and Hans Jakobsen, AU, and Jørgen Dalskov, DTU Aqua.

Technical
University
of Denmark

DTU Aqua
Øroddevej 80
DK-7900 Nykøbing M

www.aqua.dtu.dk